RSC Medicinal Chemistry

ROYAL SOCIETY OF CHEMISTRY

RESEARCH ARTICLE

Cite this: *RSC Med. Chem.*, 2023, **14**, 299

Site-directed late-stage diversification of macrocyclic nannocystins facilitating anticancer SAR and mode of action studies†

Han Zhang,‡ Yunfeng Tian,‡ Xiaoya Yuan,‡ Fei Xie, Siqi Yu, Jiayou Cai, Bin Sun, Changliang Shan* and Weicheng Zhang *

Received 26th October 2022,
Accepted 13th December 2022

DOI: 10.1039/d2md00393g

rsc.li/medchem

Nannocystins are a family of 21-membered cyclodepsipeptides with excellent anticancer activity. However, their macrocyclic architecture poses a significant challenge to structure modification. Herein, this issue is addressed by leveraging the strategy of post-macrocyclization diversification. In particular, a novel serine-incorporating nannocystin was designed so that its appending hydroxyl group could diversify into a wide variety of side chain analogues. Such effort facilitated not only structure–activity correlation at the subdomain of interest, but also the development of a macrocyclic coumarin-labeled fluorescence probe. Uptake experiments indicated good cell permeability of the probe, and endoplasmic reticulum was identified as its subcellular localization site.

Introduction

Macrocycles stand for a frontier of modern drug discovery, their large-ring architectures attaining desirable rigidity and stability, rendering a unique arrangement of functional groups to prosecute challenging biological targets.[1–3] As a privileged subset, natural macrocycles boast unmatched topology owing to long-term co-evolution with biomacromolecules.[4,5] The notion that they are not evolved as chemotherapeutics calls for structural diversification into collective analogues so as to interrogate their biologically relevant chemical space.[6] Yet a nontrivial issue hampering such synthetic campaign lies in the ring closure step, an efficiency limiting bottleneck stemming from drastic entropy loss and complicated by concentration-dependent oligomerization.[7] In this regard, it is prudent to defer diversification until after macrocyclization. Given a robust ring scaffold, step-economic derivatization at this late stage, also known as late-stage diversification,[8,9] has become a time-tested strategy to probe the structure–activity relationship (SAR) of numerous macrocyclic natural products. For instance, from preformed cyclic intermediates **1**–**6**, focused libraries were swiftly built to permute a pre-targeted subdomain of bryostatin 1,[10] palmerolide A,[11,12] epothilone,[13] largazole,[14–16] thiostrepton,[17,18] and nannocystin Ax,[19] respectively (Fig. 1). In each case, an exocyclic or embedded functional moiety (highlighted for each structure), either naturally occurring or synthetically crafted, sprouts into an array of close-in variants.

Nannocystin A (**7**, Fig. 2, left) is a 21-membered cyclodepsipeptide originally isolated from the myxobacterial genus *Nannocystis* sp.[20,21] but now accessible *via* total synthesis.[22] Its marked anticancer potency coupled with a large ring feature warrants systematic SAR exploration.[19,23–26] As discussed above, these diversity-oriented syntheses have oftentimes been encumbered by the entropy-disfavored macrocyclization step. To raise the overall efficiency, late-stage diversification is preferred in that macrocycle formation precedes divergent synthesis. In case no natural macrocycle suffices an eligible semisynthetic starting material, a custom-made counterpart shall be generated that carries a functionality at the site of interest conducive to subsequent derivatization.[27–33] While accumulated SAR results[19–21,23–26] suggest the tyrosine subunit as a viable choice for permutation, a critical relay compound is missing to pursue site-directed post-macrocyclization diversification therein. Hence, we envisioned substituting a homochiral serine for the innate tyrosine to make a designer analogue **8** (Fig. 2, right). Recent years have witnessed increasing applications of ester coupling reactions[34] in diversifying complex structures at a late stage not limited to macrocycles.[35–40] Thanks to its

The State Key Laboratory of Medicinal Chemical Biology, College of Pharmacy, and Tianjin Key Laboratory of Molecular Drug Research, Nankai University, Tianjin, People's Republic of China. E-mail: zhangweicheng@nankai.edu.cn, changliangshan@nankai.edu.cn

† Electronic supplementary information (ESI) available. See DOI: https://doi.org/10.1039/d2md00393g

‡ These authors contributed equally to this work.

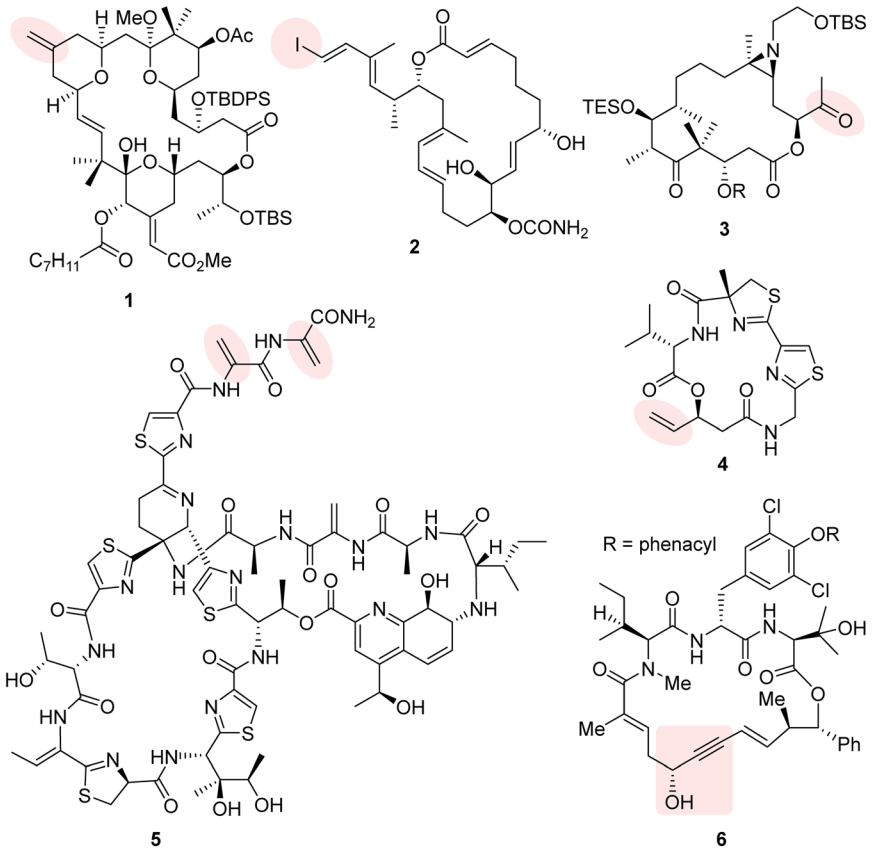

Fig. 1 Selected examples of macrocyclic intermediates 1–6 ready for late-stage diversification, each highlighted substructure denoting a diversity-conferring site.

new-appended hydroxyl handle, **8** is likewise capable of forming multiple ester derivatives for probing the chemical space efficiently. Thus obtained SAR (*vide infra*) not only validates our initial hypothesis that the tyrosine portion is editable, but also prompts creating a fluorescently labeled nannocystin. Although eukaryotic elongation factor 1A (eEF1A) has been discovered as the binding target of nannocystins,[21] their precise mode of action remains to be elucidated.[41,42] By attaching a coumarin-based reporter to the nannocystin core, we were able to characterize its uptake efficiency and subcellular localization for better mechanistic understanding.

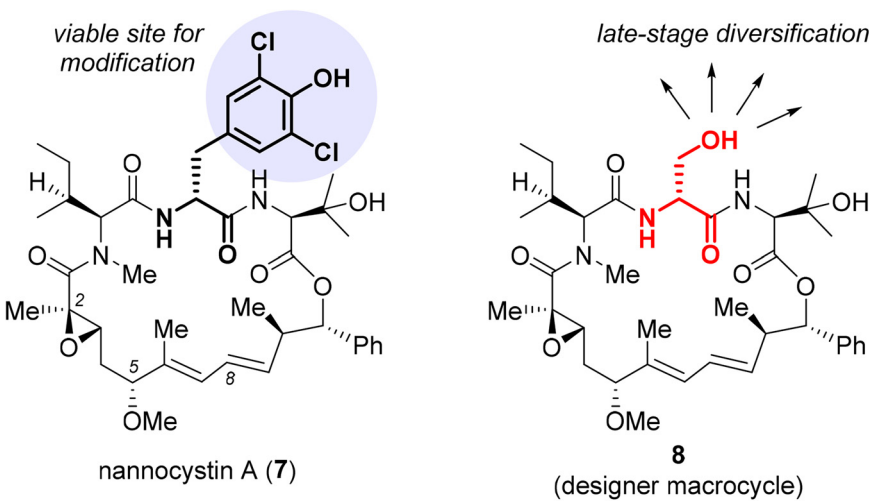

Fig. 2 Structures of naturally occurring nannocystin A (**7**) and serine-incorporating designer analogue **8**.

Results and discussion

Chemistry

Informed by relevant SAR trends,[20,21,23,26] we focused on the tyrosine subdomain for diversification. Also taking into account synthetic accessibility, we designed a serine-incorporating non-natural congener **8** amenable to site-directed post-macrocyclization diversification. Toward this end, the synthesis consists of two stages: (1) convergent synthesis of one single macrocyclic precursor and (2) divergent preparation of multiple side chain variants. In accordance with our previous total synthesis,[43] the key intermediate **8** was assembled during the first stage. As shown in Scheme 1, condensation of TBS protected D-serine methyl ester **10** with commercially available **11**, followed by Fmoc deprotection, produced dipeptide **12** in 67% yield over two steps. Amidation then took place combining **12** and epoxy acid **13** into **14**. Hydrolysis of the ester enabled amide coupling to another known building block **15**. The *seco* precursor **16** underwent a pivotal Heck macrocyclization[44,45] to afford **17** in 70% yield. Unlike Suzuki or Stille cross-coupling, a caveat regarding Heck reaction lies in the possible formation of regio- and stereoisomers prone to complicate product isolation. To our delight, the ring closure product turned out solely as an 8*E* stereoisomer, thus adding to the robustness of Heck cross-coupling in macrocycle synthesis.[46–51] Final removal of the TBS group led smoothly to **8** in 90% yield. Advancing to the second stage (Scheme 1), **8** reacted separately with different acyl donors such as acid anhydrides (for **9a** and **9d**), acyl chlorides (for **9b** and **9c**), and carboxylic acids (for **9e–9n**), under three coupling conditions (see the table inset in Scheme 1; also refer to the experimental section for synthetic details). In this way, a collection of 14 macrocyclic derivatives **9a–9n** with either an

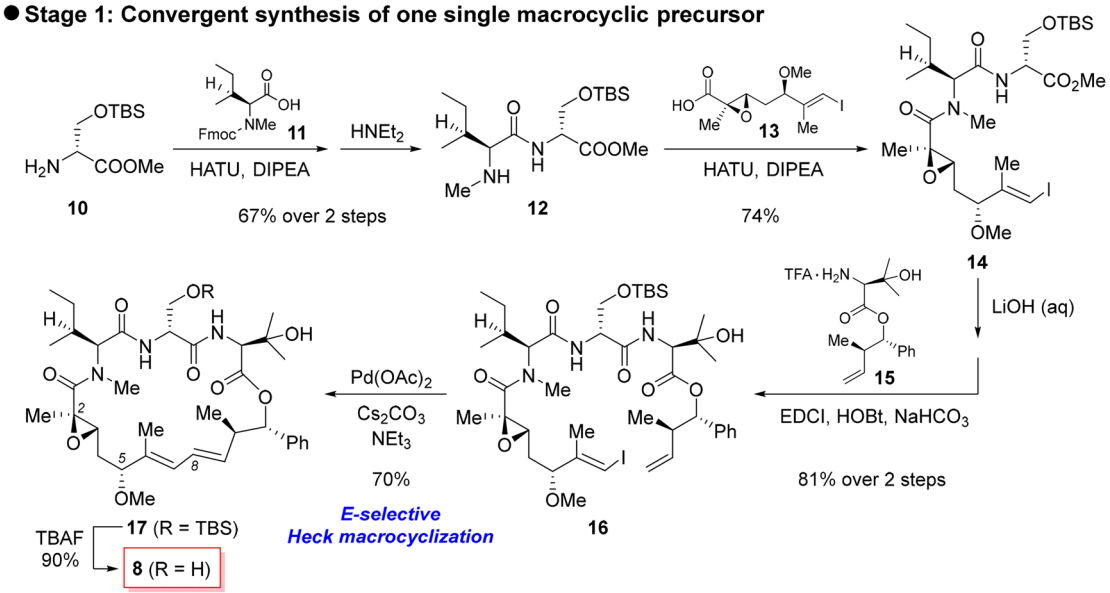

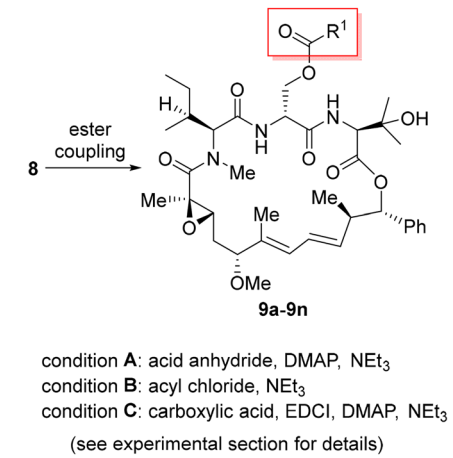

Compound	R^1	Condition	Yield (%)	Compound	R^1	Condition	Yield (%)
9a	CH_3	**A**	70	**9h**	Ph	**C**	73
9b	n-C_4H_9	**B**	60	**9i**	cyclohexyl	**C**	72
9c	n-C_9H_{19}	**B**	75	**9j**	4-pyridyl	**C**	55
9d	$CH_2CH_2CO_2H$	**A**	50	**9k**	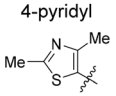	**C**	45
9e	$HC{=}CH_2$	**C**	68	**9l**		**C**	49
9f	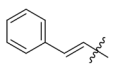	**C**	78	**9m**		**C**	60
9g	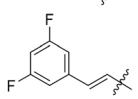	**C**	75	**9n**	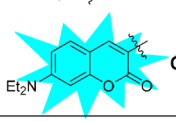	**C**	90

Scheme 1 Two-stage campaign for the efficient synthesis of macrocyclic side chain derivatives **9a–9n**.

alkyl, alkenyl, or aryl side chain R^1 were easily obtained in 45–90% yields. Among them, **9n** contains a coumarin fluorophore to facilitate mechanistic investigation using fluorescence microscopy.

Biology

Antiproliferative activities of **8** and **9a–9n**, along with reference compound **7**, were evaluated with cell counting kit-8 (CCK-8) assay against a panel of three cancer cell lines (HCT-116, HCT-8, and MDA-MB231). As shown in Table 1, our result for natural nannocystin A (entry 1) is in agreement with the literature data. For example, the IC_{50} value of **7** against HCT-116 cells was previously determined to be 1.2 nM by a thymidine pulse proliferation assay,[20] 2.6 nM by a CellTiter-Glo luminescence assay,[21] and 2.11 nM (ref. 23) or 17 nM (ref. 26) by a MTT assay. The apparent variance between these results including the current one (4.2 nM, entry 1, Table 1) is attributed quite likely to the use of different assay methods.

At the outset of this research, it was anticipated that trimming the tyrosine phenol to a much smaller serine hydroxyl, albeit at a supposedly permissive site, might have a detrimental effect on its activity, but such risk could be mitigated by ensuing ester coupling with a tunable acyl moiety. Indeed, across all three cell lines, the bare macrocyclic alcohol **8** becomes around 2–9 folds less potent than **7** (entry 2 *vs.* entry 1); once capped with an acyl group; however, the activity resumes substantially. This is especially true for colorectal carcinoma HCT-116 and HCT-8 cells, wherein over half of the side chain derivatives exhibit improved activity. Thus, our initial hypothesis that the tyrosine subdomain is modifiable has been confirmed up to this point. Interestingly, the two subsets of more active derivatives for HCT-116 (**9a–9b**, **9f–9h**, **9j–9l**) and HCT-8 (**9a–9c**, **9f–9h**, **9l–9m**) relative to **8** overlap but do not match exactly. Meanwhile, the most potent compounds for HCT-116 (**9k**) and HCT-8 (**9l**), both achieving higher activity than the natural lead **7**, are not the same. As for breast carcinoma MDA-MB231 cells, the subset of more active compounds (**9a**, **9i**, and **9k**) as well as the most potent one (**9a**) also differ from those for HCT-116 and HCT-8 cells, ostensibly owing to their different tissue origins. Such differential SAR profiles among the tested cell lines concur with a prior evaluation of **7** against 472 cell lines from the cancer cell line encyclopedia (CCLE), in which the IC_{50} values were found to be cell line-dependent, spanning two orders of magnitude (5 nM–0.5 μM) and correlating with the expression level of EEF1A1.[21] That study further proposed a binding model of **7** and its target protein eEF1A based on docking calculation.[21] Yet shortly afterwards discrepancy was spotted by an independent SAR study concerning the polyketide C5–C7 region.[19] In conjunction with the present research, these observations demonstrate the point that the efficacy of a drug to reduce cell viability, as measured phenotypically, may not correspond with its on-target binding affinity. Hence no attempt was made to interpret the data given in Table 1 in terms of on-target activity. It is worth noting that hitherto nannocystin-related SAR studies[19–21,23–26] have depended exclusively on phenotypic screening, namely, cell viability assay, rather than a target-based approach in spite of the known molecular target eEF1A. Such a seeming dilemma is at least in part due to our incomplete knowledge about the oncogenic mechanism of eEF1A.[52] Mounting evidence indicates that this multitalented protein[53] promotes malignancy through not only aberrant protein synthesis[54,55] but also a number of oncogenic signaling pathways.[56–58] Now that unable to decide whether nannocystins solely inhibit uncontrolled protein synthesis or simultaneously exert a profound impact on certain pro-tumorigenic pathway(s) mediated by eEF1A, phenotypic screening represents a more reasonable choice.[59,60] In addition, such a target-agnostic approach makes due allowance for multi-targeting mechanism (polypharmacology)[61,62] as frequently manifested by natural products.[63] This possibility for nannocystins cannot be discounted in view of two recent mode-of-action studies on nannocystin Ax, a 2*E*-alkene surrogate of **7**.[41,42] As another pertinent case, plitidepsin (dehydrodidemnin B) is a well-known macrocyclic drug approved for clinical treatment of multiple myeloma.[64] Mechanistic study showed that akin to nannocystin A, this agent targets eEF1A too,[65] notably exerting its therapeutic effect *via* not just blocking translation elongation (the canonical function of eEF1A) but also disrupting the eEF1A2-PKR (double-stranded RNA-dependent protein kinase) complex essential to the survival of cancer cells.[66] Didemnin B, the predecessor and also a reduced form of plitidepsin, was

Table 1 Antiproliferative activities of nannocystins **7**, **8**, and **9a–9n** against three cancer cell lines[a]

Entry	Compound	IC_{50}[b] (nM) HCT-116	HCT-8	MDA-MB231
1	**7**	4.2 ± 0.2	10.9 ± 0.1	15.2 ± 0.3
2	**8**	37.6 ± 0.3	32.2 ± 0.3	29.4 ± 0.3
3	**9a**	17.5 ± 0.2	24.3 ± 0.2	17.0 ± 0.6
4	**9b**	27.1 ± 0.4	18.4 ± 0.1	46.2 ± 0.2
5	**9c**	76.6 ± 0.5	16.7 ± 0.3	97.4 ± 0.4
6	**9d**	>200	115.0 ± 0.8	52.6 ± 0.2
7	**9e**	51.9 ± 0.3	35.5 ± 0.4	81.8 ± 0.5
8	**9f**	18.7 ± 0.3	27.6 ± 0.3	45.8 ± 0.1
9	**9g**	23.5 ± 0.4	24.9 ± 0.1	78.8 ± 0.6
10	**9h**	13.7 ± 0.3	23.4 ± 0.1	40.1 ± 0.1
11	**9i**	37.7 ± 0.2	44.0 ± 0.1	20.7 ± 0.4
12	**9j**	10.3 ± 0.3	57.4 ± 0.2	32.3 ± 0.2
13	**9k**	2.9 ± 0.1	60.5 ± 0.6	20.6 ± 0.4
14	**9l**	29.8 ± 0.3	2.9 ± 0.2	43.5 ± 0.1
15	**9m**	42.7 ± 0.1	19.6 ± 0.4	61.8 ± 0.3
16	**9n**	136.2 ± 1.3	52.3 ± 0.1	141.2 ± 0.3

[a] Cell histotype: HCT-116, colorectal carcinoma; HCT-8, colorectal carcinoma; MDA-MB231, breast carcinoma. [b] Determined using CCK-8 assay as triplicates in three independent experiments. Each IC_{50} value is reported as mean ± standard deviation.

found to induce rapid and extensive apoptosis through concomitant inhibition of palmitoyl-protein thioesterase 1 (PPT1) and eEF1A1.[67]

To shed light on the anticancer mechanism of nannocystins, we opted for in cellulo fluorescence imaging of a coumarin-tagged analogue **9n** (structure shown in Scheme 1). Here a fundamental design principle is to incorporate the fluorophore into the parent drug with minimal disturbance on activity.[68] Among privileged motifs for fluorescence probe design,[69] coumarin is endowed with a relatively small size, favorable photophysical properties, facile cellular uptake, low activity, and lack of intrinsic subcellular localization.[70] These advantages have encouraged the development of numerous coumarin-conjugated natural products to gain mechanistic insights,[70–73] and remarkably to boost target elucidation *via* immunoaffinity fluorescence (IAF) technique.[74–76] In the context of nannocystin research, we are interested in creating a minimally modified coumarin-bearing macrocyclic probe to visualize its intracellular distribution. Guided by the preceding SAR (Table 1), we appended 7-diethylaminocoumarin-3-carboxylic acid to **8** *via* esterification (Scheme 1), which led to **9n** in 90% yield with diminished but sufficient activity (entry 16 *vs.* entry 1, Table 1). To examine whether this probe is cell permeable, uptake experiments were conducted by treating MDA-MB231 cells with **9n** at a series of concentrations for 1 h. As shown in Fig. 3(A), the probe is capable of entering into the cells in a concentration-dependent fashion. Then, we fixed the concentration of **9n** at 1 μM and captured the intracellular fluorescence at different time periods. After 10 min treatment, a considerable amount of the probe was detected inside the cells. During the whole experimental period (0–60 min), its intracellular concentration increased with a clear time dependence (Fig. 3(B)). Moreover, repeated washing with media rendered 7-diethylaminocoumarin-3-carboxylic acid, the unconjugated control fluorophore, undetectable in the cells; by contrast, this procedure had negligible effect on intracellular accumulation of **9n**. Taken together, these observations prove satisfactory cell permeability of our designed probe.

Thus far fluorescence microscopy has become an indispensable tool to investigate the mechanism of diverse eEF1A-targeting macrocycles.[65,70,77–79] A FLIM-phasor FRET (fluorescence resonance energy transfer) approach provided concrete evidence for direct binding of coumarin-labeled plitidepsin to eEF1A2-GFP (green fluorescent protein) fusion protein.[65] Recently, single-molecule FRET (smFRET) imaging was applied to characterize the binding kinetics of ternatin derivative SR-A3 in detail for the first time.[77] Another elegant work utilized immunofluorescence analysis to establish colocalization of a rhodamine-linked fluorescence probe of BE-43547A$_2$ and eEF1A1 in the cytoplasm.[78] Nevertheless, subcellular localization of this class of targeted agents remains underexplored. To the best of our knowledge, the only one such study involved fluorescently labeled didemnin B and tamandarin A[80,81] for intracellular visualization, but with a surprising finding that both probes accumulate in the plasma membrane rather than within the cells.[70] Inspired by these pioneering efforts, we wondered subcellular localization of our probe **9n**, that is, whether it would localize preferably in a specific cellular organelle. The intracellular concentration of eEF1A was estimated to be 20 μM based on rabbit reticulocyte lysates.[82] More recently, this value has been updated as 35 μM following a proteome-wide analysis of HeLa cells.[83] Administration of **9n** at a concentration enough for fluorescence detection but far below this threshold (35 μM) ensures almost all of the probe molecules

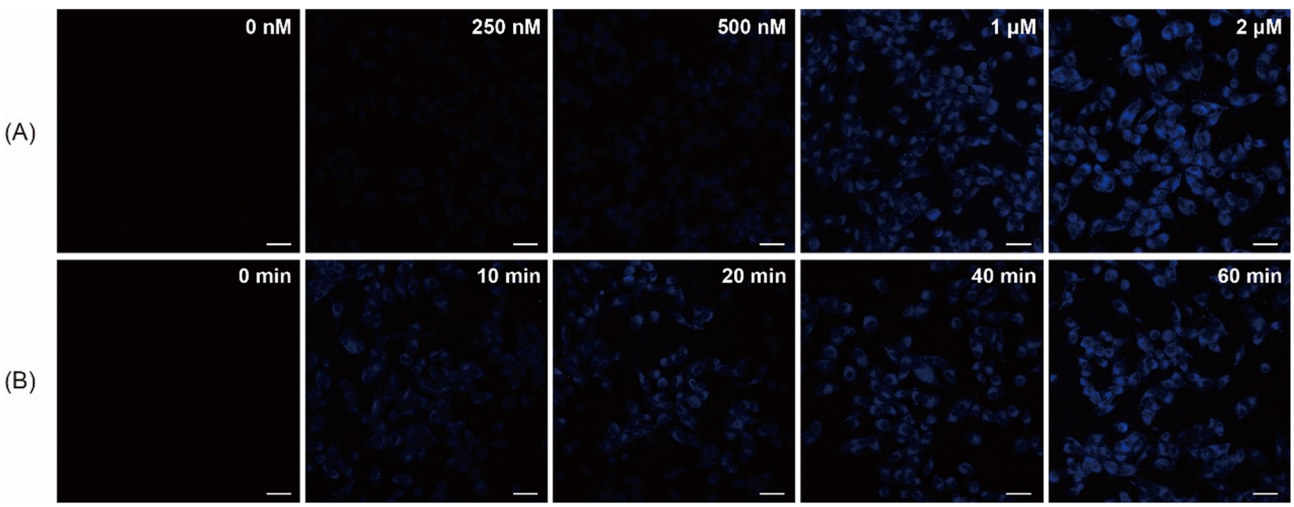

Fig. 3 Cellular uptake of coumarin-labeled nannocystin probe **9n** (λ_{ex} = 405 nm, λ_{em} = 460 nm) by MDA-MB231 cells. (A) Fluorescence images of MDA-MB231 cells treated with **9n** at different concentrations (0 nM, 250 nM, 500 nM, 1 μM, and 2 μM) for 1 h. (B) Fluorescence images of MDA-MB231 cells treated with 1 μM of **9n** for different time periods (0 min, 10 min, 20 min, 40 min, and 60 min). Scale bars, 50 μm.

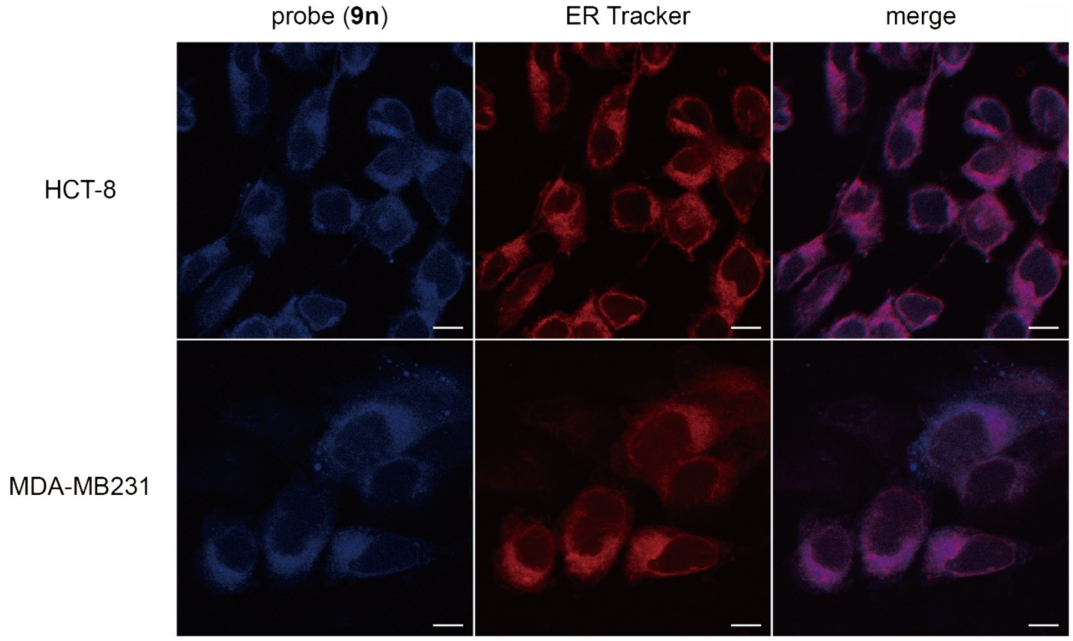

Fig. 4 Confocal fluorescence images of HCT-8 and MDA-MB231 cancer cells co-stained with nannocystin-based probe **9n** (blue, λ_{ex} = 405 nm, λ_{em} = 460 nm) and ER-Tracker (red, λ_{ex} = 587 nm, λ_{em} = 615 nm). Scale bars, 10 μm.

come into engaging their target, the eEF1A protein. Accordingly, their emission pinpoints the site where antagonistic complexation is taking place. There are two types of ribosomes in eukaryotic cells, namely, endoplasmic reticulum (ER)-bound ribosomes and cytosolic ribosomes. According to the traditional theory, protein biosynthesis is highly compartmentalized in that secretory and membrane proteins are synthesized on the former whereas cytosolic proteins on the latter.[84] However, latest studies cast doubt on this dichotomy and realized that the ER plays a central role in manufacturing not only exportable (secretory/membrane) proteins but also non-exportable (cytosolic) proteins.[85] Canonically delivering amino acyl tRNAs (aa-tRNAs) to the ribosomal A site during translation elongation, eEF1A is actively associated with the ER-bound ribosome. Hence, we suspected that ER could be the locus enriching the probe–eEF1A complex visible by fluorescence imaging. Our conjecture is additionally supported by earlier immunolocalization studies that verified the presence of eEF1A in the ER.[86–88] So we co-stained **9n**-treated HCT-8 cells with ER-Tracker Red (BODIPY TR glibenclamide). To our satisfaction, merged confocal image (Fig. 4, top right panel) indicates good overlap of red fluorescence from ER-Tracker (Fig. 4, top middle panel) and blue fluorescence from **9n** (Fig. 4, top left panel). A close match of fluorescence from ER-Tracker and **9n** was also observed in co-stained MDA-MB231 cells (Fig. 4, bottom panels). These results therefore confirm colocalization of our probe and ER, probably as a result of nannocystin–eEF1A binding to inhibit protein synthesis. It is noted, though, that the possibility of alternative mode of action cannot be ruled out considering the many moonlighting functions of eEF1A.[53,89,90] In addition to ER, eEF1A also exists in the cytosol, where it participates in translation elongation at the cytosolic ribosome apart from the ER and possibly some non-translational functions. It remains to determine whether and to what extent nannocystin interferes with the functioning of cytosolic eEF1A.[91]

Conclusions

Post-macrocyclization diversification takes advantage of a preconfigured macrocycle for efficient late-stage divergent synthesis. A prerequisite for this strategy is the presence of a diversity-conferring site, which unfortunately is not always available in macrocyclic natural products. In this situation, it is necessary to introduce such a functionality that enables facile site-directed derivatization, SAR exploration, and if feasible, mechanistic investigation. Embracing this methodology, the present work designed and synthesized a novel serine-incorporating nannocystin to displace the innate tyrosine fragment. Thus created macrocyclic alcohol was easily diversified into a library of side chain analogues *via* ester coupling to explore structure–activity correlation, which furthermore inspired developing a coumarin-tagged fluorescence probe. Fluorescence microscopy experiments showed good cell permeability of the probe and identified ER as its subcellular localization site, thereby deepening our mechanistic understanding of nannocystins. Further elucidation of the underlying mechanism of nannocystins is in progress and will be reported in due course.

Experimental section

Chemistry

General methods. All chemical reagents including solvents were purchased from commercial sources and used without purification. Unless otherwise specified, all reactions were carried out in an argon atmosphere with dry solvents under anhydrous conditions. Tetrahydrofuran (THF) was distilled immediately before use from sodium benzophenone; methylene chloride (DCM) and triethylamine (Et_3N) were distilled from calcium hydride. Reactions were monitored by thin layer chromatography (TLC) carried out on silica gel plates using UV light as a visualizing agent and aqueous phosphomolybdic acid or basic aqueous potassium permanganate as a color developing agent. Silica gel (200–300 mesh) was purchased from Qingdao Haiyang Chemical Co. for column chromatography. ^{1}H NMR and ^{13}C NMR were recorded using a Bruker AV 400 and calibrated by using internal references and solvent signals $CHCl_3$ (δ_H = 7.26 ppm, δ_C = 77.16 ppm) or DMSO (δ_H = 2.54 ppm, δ_C = 39.52 ppm). ^{1}H NMR data were reported as follows: chemical shift, multiplicity (s = singlet, d = doublet, t = triplet, q = quartet, br = broad, m = multiplet), coupling constants and integration. High-resolution mass spectra (HRMS) were detected by Varian 7.0 T FTMS. High-performance liquid chromatography (HPLC) was carried out using an Agilent 1260 infinity II system. The compounds for biological studies were eluted at a flow rate of 1.0 mL min^{-1} with water : methanol (20 : 80) within 20 min. Compounds **13** and **15** were prepared according to the literature methods.[43]

*Methyl O-(tert-butyldimethylsilyl)-N-(methyl-L-isoleucyl)-D-serinate (**12**).* DIPEA (1.49 mL, 8.56 mmol) was added to a stirred solution of **10** (1.00 g, 4.28 mmol), HATU (2.44 g, 6.42 mmol), and **11** (1.88 g, 5.13 mmol) in dry CH_2Cl_2 (9.7 mL) at 0 °C. After stirring at room temperature overnight, the reaction mixture was diluted with EtOAc (20 mL). The organic layers were washed, in turn, with aqueous HCl (1%), saturated aqueous $NaHCO_3$, and brine. After drying over anhydrous Na_2SO_4, the crude mixture was concentrated with evaporation and used directly in the next step without purification.

Diethylamine (21 mL) was added to a solution of the above-mentioned crude product in CH_2Cl_2 (42 mL) at 0 °C. The reaction mixture was stirred at room temperature for 2 h. Following evaporation of the volatile at 0 °C, 20 mL of toluene was added and the mixture was concentrated again. The concentrated crude product was purified by silica gel chromatography (petroleum ether : EtOAc = 4 : 1) to afford **12** as a colorless oil (1.04 g, 67% over two steps). ^{1}H NMR (400 MHz, $CDCl_3$) δ 7.84 (d, J = 8.1 Hz, 1H), 4.65 (d, J = 8.5 Hz, 1H), 4.05 (d, J = 9.8 Hz, 1H), 3.78 (dd, J = 9.9, 2.4 Hz, 1H), 3.69 (s, 3H), 2.84 (d, J = 4.4 Hz, 1H), 2.35 (s, 3H), 1.76 (s, 1H), 1.58–1.46 (m, 1H), 1.40–1.24 (m, 1H), 1.18–1.05 (m, 1H), 0.93 (t, J = 7.5 Hz, 3H), 0.88–0.80 (m, 12H), −0.02 (t, J = 7.8 Hz, 6H). ^{13}C NMR (101 MHz, $CDCl_3$) δ 173.26, 170.93, 70.07, 63.72, 53.74, 52.23, 38.55, 36.21, 25.67, 25.14, 18.14, 15.88, 11.92, −5.57, −5.65. HRMS–ESI (m/z): $[M + H]^+$ calcd for $C_{17}H_{36}N_2NaO_4Si^+$, 383.2337; found: 383.2340.

*Methyl O-(tert-butyldimethylsilyl)-N-(N-((2R,3S)-3-((R,E)-4-iodo-2-methoxy-3-methylbut-3-en-1-yl)-2-methyloxirane-2-carbonyl)-N-methyl-L-isoleucyl)-D-serinate (**14**).* DIPEA (0.18 mL, 1.20 mmol) was added to a stirred solution of **12** (248.8 mg, 0.69 mmol), **13** (150 mg, 0.46 mmol), and HATU (3.19 g, 8.39 mmol) in dry CH_2Cl_2 (8 mL) at 0 °C. After stirring at room temperature overnight, the reaction mixture was diluted with EtOAc (20 mL). The organic layer was washed, in turn, with aqueous HCl (1%), saturated aqueous $NaHCO_3$, and brine. After drying over anhydrous Na_2SO_4, the concentrated crude product was purified by silica gel chromatography (petroleum ether : EtOAc = 10 : 1) to afford **14** as a colorless oil (341 mg, 74%). ^{1}H NMR (400 MHz, $CDCl_3$) δ 6.76 (d, J = 7.6 Hz, 1H), 6.33 (s, 1H), 4.65 (d, J = 11.3 Hz, 1H), 4.54 (d, J = 6.7 Hz, 1H), 4.07 (d, J = 9.7 Hz, 1H), 3.87 (s, 1H), 3.78 (d, J = 9.7 Hz, 1H), 3.69 (s, 3H), 3.22 (s, 3H), 3.10 (s, 1H), 2.98 (s, 3H), 2.15 (s, 1H), 1.87 (s, 1H), 1.78 (s, 3H), 1.67 (s, 1H), 1.50 (s, 3H), 1.30 (d, J = 17.0 Hz, 1H), 1.01 (s, 1H), 0.93 (s, 3H), 0.86 (s, 12H), 0.03 (d, J = 11.9 Hz, 6H). ^{13}C NMR (101 MHz, $CDCl_3$) δ 171.37, 170.62, 169.55, 146.90, 83.89, 80.29, 63.26, 60.72, 60.62, 59.17, 56.64, 54.26, 52.38, 32.97, 30.88, 30.33, 25.86, 24.44, 18.98, 18.27, 15.88, 15.28, 10.58, −5.34, −5.56. HRMS–MALDI (m/z): $[M + Na]^+$ calcd for $C_{27}H_{49}IN_2O_7SiNa^+$, 691.2246; found: 691.2249.

*(1S,2R)-2-Methyl-1-phenylbut-3-en-1-yl (S)-2-((R)-3-((tert-butyldimethylsilyl)oxy)-2-((2S,3S)-2-((2R,3S)-3-((R,E)-4-iodo-2-methoxy-3-methylbut-3-en-1-yl)-N,2-dimethyloxirane-2-carboxamido)-3-methylpentanamido)propanamido)-3-hydroxy-3-methylbutanoate (**16**).* Aqueous LiOH (2.5 M, 0.2 mL) was added to a stirred solution of **14** (196 mg, 0.293 mmol) in THF (6 mL). After 2 h, the reaction mixture was diluted with EtOAc (20 mL). The organic layer was washed with brine and dried over anhydrous Na_2SO_4. The concentrated crude product was used directly in the next step without purification.

EDCI (60 mg, 0.313 mmol) was added to a stirred solution of the above-mentioned crude product (167 mg, 0.255 mmol), **15** (114.6 mg, 0.306 mmol), HOBt (69 mg, 0.51 mmol), and $NaHCO_3$ (32 mg, 0.381 mmol) in THF (4 mL) at 0 °C. The reaction was slowly warmed to room temperature. After stirring overnight, the reaction mixture was diluted with EtOAc (20 mL). The organic layer was washed with brine and dried over anhydrous Na_2SO_4. The concentrated crude product was purified by silica gel chromatography (petroleum ether : EtOAc = 4 : 1) to afford **16** as a colorless oil (217 mg, 81%). ^{1}H NMR (400 MHz, $CDCl_3$) δ 7.19 (dd, J = 8.9, 5.3 Hz, 5H), 7.08 (d, J = 8.7 Hz, 1H), 6.75 (d, J = 7.0 Hz, 1H), 6.24 (s, 1H), 5.54–5.43 (m, 2H), 4.89–4.81 (m, 2H), 4.44 (t, J = 9.4 Hz, 2H), 4.36–4.29 (m, 1H), 3.96 (dd, J = 10.0, 3.7 Hz, 1H), 3.77 (t, J = 6.6 Hz, 1H), 3.62 (dd, J = 9.9, 6.1 Hz, 1H), 3.14–3.07 (m, 2H), 3.05 (s, 3H), 2.97 (s, 3H), 2.74 (s, 1H), 2.66 (dd, J = 13.9, 6.9 Hz, 1H), 2.05 (s, 1H), 1.77 (s, 2H), 1.68 (s, 4H), 1.37 (d, J = 10.1 Hz, 3H), 1.03 (s, 3H), 1.00–0.96 (m, 3H), 0.95 (s, 3H), 0.80 (d, J = 8.5 Hz, 15H), 0.00 (d, J = 1.7 Hz, 6H). ^{13}C NMR

(101 MHz, $CDCl_3$) δ 171.53, 170.59, 169.97, 169.75, 146.97, 138.63, 138.10, 128.25, 127.67, 116.29, 83.75, 80.76, 80.37, 71.95, 62.79, 61.73, 60.64, 59.87, 59.44, 56.57, 54.75, 42.81, 33.08, 31.75, 31.03, 27.00, 26.76, 25.99, 24.80, 18.96, 18.37, 16.00, 15.93, 15.21, 10.76, −5.25, −5.39. HRMS–MALDI (*m*/*z*): $[M + Na]^+$ calcd for $C_{42}H_{68}IN_3O_9SiNa^+$, 936.3662; found: 936.3665.

*(1R,4S,7R,10S,13S,14R,15E,17E,19R,21S)-4-((S)-sec-Butyl)-7-(((tert-butyldimethylsilyl)oxy)methyl)-10-(2-hydroxypropan-2-yl)-19-methoxy-1,3,14,18-tetramethyl-13-phenyl-12,22-dioxa-3,6,9-triazabicyclo[19.1.0]docosa-15,17-diene-2,5,8,11-tetraone (**17**).* A mixture of $Pd(OAc)_2$ (50.2 mg, 0.224 mmol) and Cs_2CO_3 (80.9 mg, 0.249 mmol) was added to a solution of **16** (113 mg, 0.124 mmol) in 42 mL of anhydrous DMF (degassed *via* freeze–pump–thaw), followed by a solution of Et_3N (26 μL, 0.186 mmol) in 0.4 mL of DMF. The resulting solution was stirred at room temperature for 4 days. The reaction was quenched with H_2O (10 mL) and extracted with EtOAc (20 mL × 3). The combined organic layers were washed with brine, dried over anhydrous Na_2SO_4, and concentrated under reduced pressure. The crude product was purified by flash chromatography on silica gel (hexane/acetone = 8 : 1) to afford the product **17** as a white solid (68 mg, 70%). ^{1}H NMR (400 MHz, $CDCl_3$) δ 7.28–7.18 (m, 6H), 6.92 (dd, *J* = 12.0, 7.5 Hz, 2H), 6.28 (dd, *J* = 14.7, 11.2 Hz, 1H), 6.09–6.01 (m, 1H), 5.90 (s, 1H), 5.83 (dd, *J* = 15.2, 4.4 Hz, 1H), 4.63 (t, *J* = 10.0 Hz, 1H), 4.51 (d, *J* = 11.5 Hz, 1H), 4.21 (dt, *J* = 16.0, 5.9 Hz, 1H), 3.81 (dd, *J* = 9.8, 3.9 Hz, 1H), 3.64–3.55 (m, 1H), 3.49 (t, *J* = 9.1 Hz, 1H), 3.09 (s, 3H), 3.00 (s, 3H), 2.92 (d, *J* = 9.7 Hz, 1H), 2.58 (s, 1H), 2.23 (s, 1H), 2.15–2.03 (m, 3H), 1.67 (d, *J* = 6.2 Hz, 3H), 1.45 (s, 3H), 1.16 (s, 4H), 1.12 (s, 3H), 1.01 (d, *J* = 6.7 Hz, 3H), 0.80 (dd, *J* = 13.4, 6.2 Hz, 15H), −0.01 (d, *J* = 6.4 Hz, 6H). ^{13}C NMR (101 MHz, $CDCl_3$) δ 170.69, 170.43, 169.19, 169.07, 138.72, 136.14, 133.98, 129.46, 128.21, 127.79, 126.49, 126.05, 84.66, 80.03, 72.51, 63.07, 61.74, 60.39, 59.63, 58.69, 55.70, 54.66, 41.86, 31.85, 31.04, 29.83, 27.30, 26.20, 25.82, 24.28, 18.23, 15.65, 15.45, 14.12, 10.88, 10.51, 10.33, −5.33, −5.51. HRMS–MALDI (*m*/*z*): $[M + Na]^+$ calcd for $C_{42}H_{67}N_3O_9SiNa^+$, 808.4539; found: 808.4542.

*(1R,4S,7R,10S,13S,14R,15E,17E,19R,21S)-4-((S)-sec-Butyl)-7-(hydroxymethyl)-10-(2-hydroxypropan-2-yl)-19-methoxy-1,3,14,18-tetramethyl-13-phenyl-12,22-dioxa-3,6,9-triazabicyclo[19.1.0]docosa-15,17-diene-2,5,8,11-tetraone (**8**).* TBAF (0.16 mL, 1 M solution in THF) was slowly added to a solution of **17** (86.5 mg, 0.110 mmol) in anhydrous THF (4 mL) at room temperature. After stirring for 2 h, the reaction was quenched with saturated aqueous NH_4Cl (30 mL), and extracted with EtOAc (20 mL × 3). The combined organic layers were washed with brine, dried over anhydrous Na_2SO_4, and concentrated under reduced pressure. The crude product was purified by flash chromatography on silica gel (hexane/acetone = 4 : 1) to afford the product **8** as a white solid (66.5 mg, 90%). ^{1}H NMR (400 MHz, DMSO) δ 8.18 (t, *J* = 14.7 Hz, 1H), 7.48 (d, *J* = 7.6 Hz, 2H), 7.42 (s, 1H), 7.29–7.24 (m, 3H), 7.20 (t, *J* = 7.0 Hz, 1H), 6.33 (dd, *J* = 14.6, 11.6 Hz, 1H), 6.04 (td, *J* = 11.3, 7.1 Hz, 2H), 5.86 (s, 1H), 5.01 (s, 1H), 4.69–4.64 (m, 1H), 4.56 (t, *J* = 11.1 Hz, 2H), 4.48–4.39 (m, 1H), 3.59 (dd, *J* = 10.5, 2.8 Hz, 1H), 3.51 (dd, *J* = 10.9, 5.3 Hz, 1H), 3.45–3.39 (m, 1H), 3.03 (d, *J* = 7.8 Hz, 3H), 2.93 (s, 3H), 2.67–2.57 (m, 2H), 2.09 (d, *J* = 11.8 Hz, 1H), 2.04 (s, 1H), 1.95 (d, *J* = 3.6 Hz, 1H), 1.64 (s, 3H), 1.41 (s, 3H), 1.11 (s, 3H), 1.04 (d, *J* = 3.7 Hz, 1H), 0.97 (s, 3H), 0.90 (d, *J* = 6.8 Hz, 3H), 0.79 (t, *J* = 6.1 Hz, 6H).^{13}C NMR (101 MHz, DMSO) δ 170.46, 169.62, 168.88, 168.25, 139.82, 137.94, 133.40, 129.12, 127.83, 127.01, 126.04, 124.95, 83.93, 78.59, 71.77, 62.75, 61.21, 59.43, 59.16, 58.10, 55.14, 53.34, 41.71, 30.89, 30.81, 29.64, 28.19, 24.59, 23.98, 15.16, 14.83, 10.72, 10.05, 9.85. HRMS–MALDI (*m*/*z*): $[M + Na]^+$ calcd for $C_{36}H_{53}N_3O_9Na^+$, 694.3674; found: 694.3678. HPLC purity: 96.1%, t_R = 7.156 min.

*((1R,4S,7R,10S,13S,14R,15E,17E,19R,21S)-4-((S)-sec-Butyl)-10-(2-hydroxypropan-2-yl)-19-methoxy-1,3,14,18-tetramethyl-2,5,8,11-tetraoxo-13-phenyl-12,22-dioxa-3,6,9-triazabicyclo[19.1.0]docosa-15,17-dien-7-yl)methyl acetate (**9a**).* DMAP (0.6 mg, 0.005 mmol), NEt_3 (12.1 mg, 0.12 mmol), and acetic anhydride (6.12 mg, 0.06 mmol) were sequentially added to a stirred solution of **8** (33.6 mg, 0.05 mmol) in anhydrous CH_2Cl_2 (4 mL) at 0 °C. The reaction was warmed to room temperature and stirred for 8 h. The reaction was quenched with saturated aqueous NH_4Cl (2 mL) and extracted with EtOAc for three times. The combined organic layers were washed with brine, dried over anhydrous Na_2SO_4, and concentrated under reduced pressure. The crude product was purified by flash chromatography on silica gel (hexane/acetone = 6 : 1) to afford the product **9a** (25.0 mg, 70%) as a white solid. ^{1}H NMR (400 MHz, DMSO) δ 8.62 (d, *J* = 9.9 Hz, 1H), 7.92 (d, *J* = 8.5 Hz, 1H), 7.53 (d, *J* = 7.5 Hz, 2H), 7.32 (t, *J* = 7.4 Hz, 2H), 7.28–7.23 (m, 1H), 6.43–6.31 (m, 1H), 6.16–6.06 (m, 2H), 5.93 (s, 1H), 5.12 (s, 1H), 4.77 (dd, *J* = 13.5, 5.7 Hz, 1H), 4.63 (d, *J* = 9.8 Hz, 2H), 4.13–4.01 (m, 2H), 3.64 (d, *J* = 10.0 Hz, 1H), 3.09 (s, 3H), 3.01 (s, 3H), 2.67 (d, *J* = 8.6 Hz, 2H), 2.12 (t, *J* = 12.4 Hz, 1H), 1.97 (s, 1H), 1.92 (s, 3H), 1.68 (s, 3H), 1.45 (s, 3H), 1.30 (s, 1H), 1.12 (s, 3H), 1.00 (s, 3H), 0.95 (d, *J* = 6.7 Hz, 4H), 0.83 (t, *J* = 7.2 Hz, 7H). ^{13}C NMR (101 MHz, DMSO) δ 170.29, 169.90, 169.65, 168.79, 167.84, 139.84, 138.10, 133.47, 129.04, 127.82, 127.03, 126.06, 124.94, 83.93, 78.72, 71.82, 63.90, 61.22, 59.52, 58.90, 58.18, 55.17, 50.19, 41.86, 31.05, 30.79, 29.70, 28.05, 24.46, 24.07, 20.57, 14.89, 14.80, 10.74, 10.09, 9.77. HRMS–ESI (*m*/*z*): $[M + H]^+$ calcd for $C_{38}H_{56}N_3O_{10}^+$, 714.3960; found: 714.3949. HPLC purity: 96.2%, t_R = 7.854 min.

*((1R,4S,7R,10S,13S,14R,15E,17E,19R,21S)-4-((S)-sec-Butyl)-10-(2-hydroxypropan-2-yl)-19-methoxy-1,3,14,18-tetramethyl-2,5,8,11-tetraoxo-13-phenyl-12,22-dioxa-3,6,9-triazabicyclo[19.1.0]docosa-15,17-dien-7-yl)methyl pentanoate (**9b**).* NEt_3 (16.2 mg, 0.16 mmol) and *N*-pentanoyl chloride (19.3 mg, 0.16 mmol) were sequentially added to a stirred solution of **8** (33.6 mg, 0.05 mmol) in anhydrous CH_2Cl_2 (4 mL) at 0 °C. The reaction was warmed to room temperature and stirred for 8 h. The reaction was quenched with saturated aqueous NH_4Cl (2 mL) and extracted with EtOAc for three times. The combined organic layers were washed with brine, dried over anhydrous Na_2SO_4, and concentrated

under reduced pressure. The crude product was purified by flash chromatography on silica gel (hexane/acetone = 6 : 1) to afford the product **9b** (22.7 mg, 60%) as a white solid. ^{1}H NMR (400 MHz, DMSO) δ 8.63 (d, J = 9.8 Hz, 1H), 7.83 (d, J = 8.3 Hz, 1H), 7.53 (d, J = 7.4 Hz, 2H), 7.32 (t, J = 7.4 Hz, 2H), 7.25 (t, J = 6.9 Hz, 1H), 6.37 (dd, J = 14.5, 11.7 Hz, 1H), 6.15–6.06 (m, 2H), 5.93 (s, 1H), 5.13 (s, 1H), 4.78–4.71 (m, 1H), 4.62 (dd, J = 10.5, 8.8 Hz, 2H), 4.11 (qd, J = 11.1, 5.2 Hz, 2H), 3.64 (dd, J = 10.5, 3.0 Hz, 1H), 3.09 (s, 3H), 3.00 (s, 3H), 2.68 (dd, J = 9.9, 1.9 Hz, 2H), 2.24–2.17 (m, 2H), 2.12 (t, J = 9.3 Hz, 1H), 2.03–1.94 (m, 1H), 1.68 (s, 3H), 1.45 (s, 4H), 1.30–1.19 (m, 3H), 1.12 (s, 3H), 1.00 (s, 3H), 0.95 (d, J = 6.8 Hz, 4H), 0.86–0.79 (m, 11H). ^{13}C NMR (101 MHz, DMSO) δ 172.47, 170.30, 169.66, 168.67, 167.76, 139.83, 138.07, 133.43, 129.07, 127.83, 127.03, 126.05, 124.92, 83.93, 78.70, 71.78, 63.83, 61.20, 59.50, 58.92, 58.16, 55.16, 50.34, 41.84, 33.08, 30.94, 30.82, 29.67, 28.08, 26.38, 24.46, 24.02, 21.59, 14.92, 14.80, 13.58, 10.72, 10.04, 9.75. HRMS–MALDI (m/z): $[M + Na]^+$ calcd for $C_{41}H_{61}N_3O_{10}Na^+$, 778.4249; found: 778.4252. HPLC purity: 95.7%, t_R = 11.231 min.

*((1R,4S,7R,10S,13S,14R,15E,17E,19R,21S)-4-((S)-sec-Butyl)-10-(2-hydroxypropan-2-yl)-19-methoxy-1,3,14,18-tetramethyl-2,5,8,11-tetraoxo-13-phenyl-12,22-dioxa-3,6,9-triazabicyclo[19.1.0]docosa-15,17-dien-7-yl)methyl decanoate (**9c**).* The title compound was synthesized from **8** following the general procedure described for **9b**. Flash column chromatography with hexane and acetone (6 : 1) as eluants afforded the product **9c** in 75% yield as a white solid. ^{1}H NMR (400 MHz, DMSO) δ 8.56 (d, J = 9.8 Hz, 1H), 7.77 (d, J = 8.3 Hz, 1H), 7.47 (d, J = 7.4 Hz, 2H), 7.25 (t, J = 7.7 Hz, 2H), 7.18 (t, J = 7.2 Hz, 1H), 6.31 (dd, J = 15.2, 10.9 Hz, 1H), 6.09–6.00 (m, 2H), 5.87 (s, 1H), 5.06 (s, 1H), 4.71–4.65 (m, 1H), 4.56 (dd, J = 10.4, 8.9 Hz, 2H), 4.04 (ddd, J = 16.9, 11.0, 5.1 Hz, 2H), 3.57 (dd, J = 10.5, 2.9 Hz, 1H), 3.02 (s, 4H), 2.93 (s, 3H), 2.61 (dd, J = 9.9, 1.8 Hz, 2H), 2.16–2.08 (m, 2H), 2.04 (d, J = 11.4 Hz, 1H), 1.97–1.88 (m, 1H), 1.62 (s, 3H), 1.40 (d, J = 8.1 Hz, 6H), 1.16 (s, 10H), 1.05 (s, 3H), 0.93 (s, 3H), 0.89 (d, J = 6.8 Hz, 4H), 0.80–0.74 (m, 11H).^{13}C NMR (101 MHz, DMSO) δ 172.47, 170.29, 169.65, 168.67, 167.76, 139.83, 138.08, 133.43, 129.09, 127.83, 127.02, 126.05, 124.92, 83.95, 78.70, 71.79, 63.83, 61.20, 59.49, 58.94, 58.16, 55.15, 50.35, 41.85, 33.36, 31.32, 30.96, 30.83, 29.66, 28.87, 28.70, 28.44, 28.10, 24.47, 24.28, 24.04, 22.14, 14.93, 14.80, 13.99, 10.71, 10.05, 9.75.HRMS–MALDI (m/z): $[M + Na]^+$ calcd for $C_{46}H_{71}N_3O_{10}Na^+$, 848.5032; found: 848.5035. HPLC purity: 95.5%, t_R = 18.157 min.

*4-(((1R,4S,7R,10S,13S,14R,15E,17E,19R,21S)-4-((S)-sec-Butyl)-10-(2-hydroxypropan-2-yl)-19-methoxy-1,3,14,18-tetramethyl-2,5,8,11-tetraoxo-13-phenyl-12,22-dioxa-3,6,9-triazabicyclo[19.1.0]docosa-15,17-dien-7-yl)methoxy)-4-oxobutanoic acid (**9d**).* The title compound was synthesized from **8** following the general procedure described for **9a**. Flash column chromatography with hexane and acetone (6 : 1) as eluants afforded the product **9d** in 50% yield as a white solid. ^{1}H NMR (400 MHz, DMSO) δ 12.23 (s, 1H), 8.61 (d, J = 9.8 Hz, 1H), 7.90 (d, J = 8.6 Hz, 1H), 7.52 (d, J = 7.5 Hz, 2H), 7.30 (t, J = 7.4 Hz, 2H), 7.23 (t, J = 7.2 Hz, 1H), 6.35 (dd, J = 14.4, 11.5 Hz, 1H), 6.13–6.04 (m, 2H), 5.92 (s, 1H), 5.10 (s, 1H), 4.77–4.71 (m, 1H), 4.64–4.58 (m, 2H), 4.07 (td, J = 10.8, 6.0 Hz, 2H), 3.62 (dd, J = 10.4, 2.9 Hz, 1H), 3.07 (s, 4H), 2.99 (s, 3H), 2.65 (d, J = 8.0 Hz, 2H), 2.42–2.39 (m, 4H), 2.10 (s, 1H), 1.96 (s, 1H), 1.66 (s, 3H), 1.44 (s, 3H), 1.12 (s, 1H), 1.10 (s, 2H), 0.98 (s, 3H), 0.94 (d, J = 6.8 Hz, 3H), 0.81 (dd, J = 10.5, 6.9 Hz, 8H).^{13}C NMR (101 MHz, DMSO) δ 173.27, 171.72, 170.29, 169.64, 168.78, 167.78, 139.84, 138.09, 133.46, 129.05, 127.83, 127.03, 126.06, 124.94, 83.93, 78.71, 71.81, 64.08, 61.21, 59.52, 58.93, 58.19, 55.17, 50.22, 41.86, 31.08, 29.70, 29.62, 28.56, 28.50, 28.09, 24.47, 24.06, 14.87, 14.79, 10.73, 10.14, 9.77. HRMS–ESI (m/z): $[M + H]^+$ calcd for $C_{40}H_{58}N_3O_{12}^+$, 772.4015; found: 772.4006. HPLC purity: 95.5%, t_R = 7.185 min.

*((1R,4S,7R,10S,13S,14R,15E,17E,19R,21S)-4-((S)-sec-Butyl)-10-(2-hydroxypropan-2-yl)-19-methoxy-1,3,14,18-tetramethyl-2,5,8,11-tetraoxo-13-phenyl-12,22-dioxa-3,6,9-triazabicyclo[19.1.0]docosa-15,17-dien-7-yl)methyl acrylate (**9e**).* DMAP (0.6 mg, 0.005 mmol), NEt_3 (12.1 mg, 0.12 mmol), EDCI (13.4 mg, 0.07 mmol), and acrylic acid (4.3 mg, 0.06 mmol) were sequentially added to a stirred solution of **8** (33.6 mg, 0.05 mmol) in anhydrous CH_2Cl_2 (4 mL) at 0 °C. The reaction was warmed to room temperature and stirred for 8 h. The reaction was quenched with saturated aqueous NH_4Cl (2 mL) and extracted with EtOAc for three times. The combined organic layers were washed with brine, dried over anhydrous Na_2SO_4, and concentrated under reduced pressure. The crude product was purified by flash chromatography on silica gel (hexane/acetone = 6 : 1) to afford the product **9e** (24.7 mg, 68%) as a white solid. ^{1}H NMR (400 MHz, $CDCl_3$) δ 7.35 (d, J = 13.0 Hz, 4H), 7.29 (d, J = 4.7 Hz, 1H), 7.03 (d, J = 6.4 Hz, 1H), 6.87 (d, J = 8.8 Hz, 1H), 6.35 (dd, J = 10.6, 6.7 Hz, 2H), 6.14 (d, J = 10.7 Hz, 1H), 6.02–5.84 (m, 3H), 5.79 (d, J = 10.5 Hz, 1H), 4.74 (dd, J = 23.5, 7.4 Hz, 2H), 4.53 (d, J = 11.5 Hz, 1H), 4.29 (ddd, J = 28.7, 11.2, 5.2 Hz, 2H), 3.68 (d, J = 7.6 Hz, 1H), 3.21 (d, J = 4.8 Hz, 1H), 3.18 (s, 3H), 3.10 (s, 3H), 3.01 (d, J = 9.7 Hz, 1H), 2.68 (s, 1H), 2.19–2.08 (m, 2H), 1.79 (s, 1H), 1.74 (s, 3H), 1.53 (s, 3H), 1.24 (s, 3H), 1.15 (s, 3H), 1.09 (d, J = 6.8 Hz, 3H), 0.99–0.93 (m, 2H), 0.87 (dd, J = 17.1, 6.7 Hz, 6H) ^{13}C NMR (101 MHz, $CDCl_3$) δ 170.98, 170.23, 169.22, 168.06, 165.60, 138.62, 136.38, 134.15, 132.12, 129.22, 128.37, 128.02, 127.63, 126.76, 126.21, 84.57, 80.36, 72.58, 64.12, 61.94, 60.79, 60.13, 58.81, 55.98, 51.92, 42.03, 31.79, 31.47, 30.14, 27.41, 26.48, 24.51, 15.65, 15.51, 11.28, 10.81, 10.65. HRMS–MALDI (m/z): $[M + Na]^+$ calcd for $C_{39}H_{55}N_3O_{10}Na^+$, 748.3780; found: 748.3782. HPLC purity: 96.2%, t_R = 8.182 min.

*((1R,4S,7R,10S,13S,14R,15E,17E,19R,21S)-4-((S)-sec-Butyl)-10-(2-hydroxypropan-2-yl)-19-methoxy-1,3,14,18-tetramethyl-2,5,8,11-tetraoxo-13-phenyl-12,22-dioxa-3,6,9-triazabicyclo[19.1.0]docosa-15,17-dien-7-yl)methyl cinnamate (**9f**).* The title compound was synthesized from **8** and cinnamic acid following the general procedure described for **9e**. Flash column chromatography with hexane and acetone (6 : 1) as eluants afforded the product **9f** in 78% yield as a

white solid. ^{1}H NMR (400 MHz, DMSO) δ 8.71 (d, J = 9.6 Hz, 1H), 7.96 (d, J = 8.4 Hz, 1H), 7.68 (d, J = 16.9 Hz, 3H), 7.59 (d, J = 7.0 Hz, 2H), 7.50 (s, 3H), 7.37 (d, J = 6.4 Hz, 2H), 7.32 (d, J = 6.5 Hz, 1H), 6.54 (d, J = 15.6 Hz, 1H), 6.49–6.38 (m, 1H), 6.16 (t, J = 12.4 Hz, 2H), 5.99 (s, 1H), 5.17 (s, 1H), 4.93 (s, 1H), 4.70 (d, J = 9.6 Hz, 2H), 4.31 (s, 2H), 3.71 (d, J = 9.9 Hz, 2H), 3.15 (s, 3H), 3.07 (s, 3H), 2.76 (d, J = 9.9 Hz, 3H), 2.17 (s, 1H), 2.07 (s, 1H), 1.74 (s, 3H), 1.51 (s, 3H), 1.35 (s, 1H), 1.19 (s, 3H), 1.06 (s, 3H), 1.02 (d, J = 5.7 Hz, 3H), 0.88 (d, J = 5.4 Hz, 6H). ^{13}C NMR (101 MHz, DMSO) δ 170.26, 169.73, 168.74, 167.76, 165.58, 144.86, 139.78, 137.94, 133.84, 133.45, 130.63, 129.35, 129.04, 128.21, 127.80, 127.00, 126.03, 124.95, 117.47, 83.82, 78.69, 71.71, 64.27, 61.14, 59.60, 58.98, 58.13, 55.14, 50.45, 41.80, 30.95, 30.82, 29.68, 28.07, 24.61, 23.98, 14.97, 14.78, 10.77, 10.03, 9.83. HRMS–MALDI (m/z): $[M + Na]^+$ calcd for $C_{45}H_{59}N_3O_{10}Na^+$, 824.4093; found: 824.4098. HPLC purity: 95.6%, t_R = 11.221 min.

*((1R,4S,7R,10S,13S,14R,15E,17E,19R,21S)-4-((S)-sec-Butyl)-10-(2-hydroxypropan-2-yl)-19-methoxy-1,3,14,18-tetramethyl-2,5,8,11-tetraoxo-13-phenyl-12,22-dioxa-3,6,9-triazabicyclo[19.1.0]docosa-15,17-dien-7-yl)methyl (E)-3-(3,5-difluorophenyl)acrylate (**9g**).* The title compound was synthesized from **8** and (*E*)-3-(3,5-difluorophenyl)acrylic acid following the general procedure described for **9e**. Flash column chromatography with hexane and acetone (6 : 1) as eluants afforded the product **9g** in 75% yield as a white solid. ^{1}H NMR (400 MHz, DMSO) δ 8.66 (d, J = 9.6 Hz, 1H), 7.97 (d, J = 8.7 Hz, 1H), 7.60–7.50 (m, 3H), 7.31 (t, J = 7.3 Hz, 2H), 7.24 (t, J = 8.5 Hz, 3H), 6.54 (d, J = 16.5 Hz, 1H), 6.41–6.32 (m, 1H), 6.10 (t, J = 12.8 Hz, 2H), 5.93 (s, 1H), 5.10 (s, 1H), 4.87 (s, 1H), 4.64 (dd, J = 10.5, 4.2 Hz, 2H), 4.25 (d, J = 6.6 Hz, 2H), 3.64 (d, J = 8.7 Hz, 1H), 3.08 (s, 3H), 3.00 (s, 3H), 2.67 (d, J = 8.8 Hz, 2H), 2.11 (t, J = 12.0 Hz, 1H), 1.98 (s, 1H), 1.68 (s, 3H), 1.44 (s, 3H), 1.29 (s, 3H), 1.25 (s, 1H), 1.13 (s, 3H), 0.99 (s, 3H), 0.95 (d, J = 6.7 Hz, 3H), 0.83–0.79 (m, 6H). ^{13}C NMR (101 MHz, DMSO) δ 170.21, 169.63, 168.77, 167.65, 165.19, 163.11 (d, J = 6.6 Hz), 160.56 (d, J = 6.6 Hz), 139.77, 137.98, 133.43, 131.70 (t, J = 11.0 Hz), 130.39, 128.93, 127.77, 126.97, 126.01, 124.92, 123.34 (t, J = 9.0 Hz), 112.43 (d, J = 24.8 Hz), 83.86, 78.69, 71.74, 64.48, 61.14, 59.53, 58.92, 58.11, 55.13, 50.28, 41.81, 31.13, 30.75, 29.81, 28.98, 28.01, 24.46, 23.99, 22.07, 14.83, 14.77, 10.73, 10.01, 9.77. ^{19}F NMR (376 MHz, DMSO) δ −111.25. HRMS–MALDI (m/z): $[M + Na]^+$ calcd for $C_{45}H_{57}N_3O_{10}Na^+$, 860.3904; found: 860.3910. HPLC purity: 95.8%, t_R = 10.917 min.

*((1R,4S,7R,10S,13S,14R,15E,17E,19R,21S)-4-((S)-sec-Butyl)-10-(2-hydroxypropan-2-yl)-19-methoxy-1,3,14,18-tetramethyl-2,5,8,11-tetraoxo-13-phenyl-12,22-dioxa-3,6,9-triazabicyclo[19.1.0]docosa-15,17-dien-7-yl)methyl benzoate (**9h**).* The title compound was synthesized from **8** and benzoic acid following the general procedure described for **9e**. Flash column chromatography with hexane and acetone (6 : 1) as eluants afforded the product **9h** in 73% yield as a white solid. ^{1}H NMR (400 MHz, DMSO) δ 8.72 (d, J = 10.0 Hz, 1H), 8.01 (d, J = 8.0 Hz, 1H), 7.94 (d, J = 7.3 Hz, 2H), 7.66 (d, J = 7.3 Hz, 1H), 7.53 (dd, J = 12.9, 7.6 Hz, 4H), 7.32 (t, J = 7.3 Hz, 2H), 7.26 (d, J = 7.0 Hz, 1H), 6.43–6.33 (m, 1H), 6.12 (t, J = 13.0 Hz, 2H), 5.95 (s, 1H), 5.12 (s, 1H), 4.94 (s, 1H), 4.65 (dd, J = 10.4, 6.2 Hz, 2H), 4.38 (d, J = 13.5 Hz, 2H), 3.65 (d, J = 8.0 Hz, 1H), 3.10 (s, 4H), 3.02 (s, 3H), 2.70 (d, J = 10.6 Hz, 2H), 2.18–2.09 (m, 1H), 2.00 (s, 2H), 1.69 (s, 3H), 1.45 (d, J = 8.6 Hz, 3H), 1.27 (s, 2H), 1.07 (s, 3H), 0.96 (d, J = 7.2 Hz, 5H), 0.81 (s, 3H), 0.76 (d, J = 6.4 Hz, 3H). ^{13}C NMR (101 MHz, DMSO) δ 170.35, 169.69, 168.81, 167.68, 165.34, 139.85, 138.13, 133.52, 133.42, 129.34, 129.31, 129.12, 128.62, 127.83, 127.03, 126.04, 124.89, 83.95, 78.70, 71.71, 65.24, 61.24, 59.54, 58.94, 58.18, 55.15, 50.44, 41.86, 31.01, 30.82, 29.71, 28.05, 24.50, 24.02, 14.93, 14.81, 10.71, 10.11, 9.71. HRMS–MALDI (m/z): $[M + Na]^+$ calcd for $C_{43}H_{57}N_3O_{10}Na^+$, 798.3936; found: 798.3940. HPLC purity: 95.6%, t_R = 10.044 min.

*((1R,4S,7R,10S,13S,14R,15E,17E,19R,21S)-4-((S)-sec-Butyl)-10-(2-hydroxypropan-2-yl)-19-methoxy-1,3,14,18-tetramethyl-2,5,8,11-tetraoxo-13-phenyl-12,22-dioxa-3,6,9-triazabicyclo[19.1.0]docosa-15,17-dien-7-yl)methyl cyclohexanecarboxylate (**9i**).* The title compound was synthesized from **8** and cyclohexanecarboxylic acid following the general procedure described for **9e**. Flash column chromatography with hexane and acetone (6 : 1) as eluants afforded the product **9i** in 72% yield as a white solid. ^{1}H NMR (400 MHz, $CDCl_3$) δ 7.38–7.33 (m, 4H), 7.31–7.27 (m, 1H), 7.03 (d, J = 6.7 Hz, 1H), 6.81 (d, J = 9.0 Hz, 1H), 6.35 (dd, J = 14.7, 11.5 Hz, 1H), 6.14 (d, J = 10.7 Hz, 1H), 5.99 (s, 1H), 5.92 (dd, J = 15.3, 4.6 Hz, 1H), 4.76–4.65 (m, 2H), 4.52 (d, J = 11.5 Hz, 1H), 4.29 (dd, J = 11.3, 5.4 Hz, 1H), 4.14 (dd, J = 11.3, 4.4 Hz, 1H), 3.67 (dd, J = 10.5, 2.6 Hz, 1H), 3.17 (s, 3H), 3.09 (s, 3H), 2.98 (d, J = 8.2 Hz, 1H), 2.64 (d, J = 11.8 Hz, 1H), 2.21 (ddd, J = 33.6, 16.7, 7.8 Hz, 3H), 1.83 (d, J = 12.5 Hz, 2H), 1.73 (d, J = 7.9 Hz, 3H), 1.73–1.66 (m, 2H), 1.61 (s, 2H), 1.55–1.51 (m, 3H), 1.42–1.30 (m, 4H), 1.25 (s, 4H), 1.20 (d, J = 4.9 Hz, 1H), 1.17 (s, 3H), 1.10 (d, J = 6.8 Hz, 3H), 1.02–0.93 (m, 2H), 0.87 (dd, J = 11.9, 6.7 Hz, 6H). ^{13}C NMR (101 MHz, $CDCl_3$) δ 175.73, 170.92, 170.38, 169.01, 168.16, 138.79, 136.54, 134.12, 129.49, 128.37, 127.97, 126.68, 126.08, 84.70, 80.39, 72.65, 63.78, 61.91, 60.75, 60.04, 58.80, 55.90, 52.11, 43.03, 42.04, 31.83, 31.40, 30.11, 29.04, 28.90, 27.28, 26.45, 25.74, 25.45, 25.40, 24.47, 15.63, 15.52, 11.08, 10.70, 10.42. HRMS–MALDI (m/z): $[M + Na]^+$ calcd for $C_{43}H_{63}N_3O_{10}Na^+$, 804.4406; found: 804.4410. HPLC purity: 95.1%, t_R = 12.807 min.

*((1R,4S,7R,10S,13S,14R,15E,17E,19R,21S)-4-((S)-sec-Butyl)-10-(2-hydroxypropan-2-yl)-19-methoxy-1,3,14,18-tetramethyl-2,5,8,11-tetraoxo-13-phenyl-12,22-dioxa-3,6,9-triazabicyclo[19.1.0]docosa-15,17-dien-7-yl)methyl isonicotinate (**9j**).* The title compound was synthesized from **8** and isonicotinic acid following the general procedure described for **9e**. Flash column chromatography with hexane and acetone (6 : 1) as eluants afforded the product **9j** in 55% yield as a white solid. ^{1}H NMR (400 MHz, DMSO) δ 8.80 (d, J = 4.3 Hz, 2H), 8.72 (d, J = 9.7 Hz, 1H), 8.07 (d, J = 8.4 Hz, 1H), 7.78 (d, J = 4.7 Hz, 2H), 7.52 (d, J = 7.4 Hz, 1H), 7.35–7.27 (m, 3H), 7.24 (d, J = 6.6 Hz, 1H), 6.42–6.30 (m, 1H), 6.09 (dd, J = 18.1, 6.9 Hz, 2H), 5.93 (s, 1H), 5.10 (s, 1H), 4.91 (d, J = 16.6 Hz, 1H), 4.64 (d, J = 10.5 Hz, 2H), 4.42 (s, 2H), 3.63 (d, J = 10.6

Hz, 1H), 3.09 (d, J = 14.8 Hz, 4H), 3.00 (s, 3H), 2.67 (d, J = 9.7 Hz, 2H), 2.10 (t, J = 12.0 Hz, 1H), 1.98 (s, 1H), 1.67 (s, 3H), 1.48–1.41 (m, 4H), 1.28 (s, 1H), 1.04 (d, J = 7.8 Hz, 3H), 0.94 (d, J = 6.0 Hz, 5H), 0.82–0.77 (m, 4H), 0.73 (d, J = 6.3 Hz, 3H). ^{13}C NMR (101 MHz, DMSO) δ 170.32, 169.69, 168.86, 167.53, 164.20, 150.70, 139.82, 138.10, 136.53, 133.44, 129.07, 127.83, 127.04, 126.04, 124.90, 122.63, 83.91, 78.72, 71.68, 65.78, 61.22, 59.56, 58.90, 58.19, 55.16, 50.30, 41.86, 31.06, 29.71, 29.04, 27.99, 24.56, 24.02, 14.91, 14.80, 10.73, 10.12, 9.74. HRMS–MALDI (m/z): $[M + Na]^+$ calcd for $C_{42}H_{56}N_4O_{10}Na^+$, 799.3889; found: 799.3893. HPLC purity: 96.5%, t_R = 8.168 min.

*((1R,4S,7R,10S,13S,14R,15E,17E,19R,21S)-4-((S)-sec-Butyl)-10-(2-hydroxypropan-2-yl)-19-methoxy-1,3,14,18-tetramethyl-2,5,8,11-tetraoxo-13-phenyl-12,22-dioxa-3,6,9-triazabicyclo[19.1.0]docosa-15,17-dien-7-yl)methyl 2,4-dimethylthiazole-5-carboxylate (**9k**).* The title compound was synthesized from **8** and 2,4-dimethylthiazole-5-carboxylic acid following the general procedure described for **9e**. Flash column chromatography with hexane and acetone (6 : 1) as eluants afforded the product **9k** in 45% yield as a white solid. ^{1}H NMR (400 MHz, MeOD) δ 7.47 (d, J = 7.3 Hz, 2H), 7.32 (t, J = 6.9 Hz, 3H), 7.25 (d, J = 6.9 Hz, 1H), 6.48–6.39 (m, 1H), 6.15 (d, J = 10.6 Hz, 1H), 6.04 (d, J = 23.1 Hz, 2H), 4.71–4.62 (m, 3H), 4.39 (d, J = 9.9 Hz, 1H), 3.70 (d, J = 10.5 Hz, 1H), 3.18 (d, J = 9.7 Hz, 4H), 3.08 (s, 3H), 2.90 (d, J = 10.1 Hz, 1H), 2.69 (d, J = 6.4 Hz, 1H), 2.66 (s, 3H), 2.61 (s, 3H), 2.18 (dd, J = 23.6, 14.9 Hz, 3H), 1.73 (s, 3H), 1.52 (s, 3H), 1.29 (m, 1H),1.24 (s, 3H), 1.10 (s, 3H), 1.07 (d, J = 6.4 Hz, 3H), 0.92–0.85 (m, 8H). ^{13}C NMR (101 MHz, MeOD) δ 172.88, 172.18, 171.55, 170.66, 169.18, 162.57, 161.30, 140.92, 138.66, 134.45, 131.33, 129.05, 128.38, 127.48, 126.59, 122.17, 85.91, 80.93, 73.39, 65.99, 62.71, 61.55, 61.19, 59.92, 55.95, 52.95, 43.45, 32.44, 32.31, 30.73, 28.56, 25.47, 25.30, 19.02, 17.24, 15.83, 15.52, 10.80, 10.49, 10.37.HRMS–MALDI (m/z): $[M + Na]^+$ calcd for $C_{42}H_{58}N_4O_{10}Na^+$, 833.3766; found: 833.3770. HPLC purity: 95.8%, t_R = 9.199 min.

*((1R,4S,7R,10S,13S,14R,15E,17E,19R,21S)-4-((S)-sec-Butyl)-10-(2-hydroxypropan-2-yl)-19-methoxy-1,3,14,18-tetramethyl-2,5,8,11-tetraoxo-13-phenyl-12,22-dioxa-3,6,9-triazabicyclo[19.1.0]docosa-15,17-dien-7-yl)methyl cyclobut-1-ene-1-carboxylate (**9l**).* The title compound was synthesized from **8** and cyclobut-1-ene-1-carboxylic acid following the general procedure described for **9e**. Flash column chromatography with hexane and acetone (6 : 1) as eluants afforded the product **9l** in 49% yield as a white solid. ^{1}H NMR (400 MHz, DMSO) δ 8.60 (d, J = 9.8 Hz, 1H), 7.82 (d, J = 8.3 Hz, 1H), 7.53 (d, J = 7.5 Hz, 2H), 7.32 (t, J = 7.5 Hz, 3H), 7.26 (d, J = 7.3 Hz, 1H), 6.37 (dd, J = 14.6, 11.7 Hz, 1H), 6.09 (dd, J = 19.9, 8.0 Hz, 2H), 5.93 (s, 1H), 5.12 (s, 1H), 4.78–4.72 (m, 1H), 4.61 (dd, J = 10.5, 8.0 Hz, 2H), 4.12 (ddd, J = 17.1, 11.0, 5.2 Hz, 2H), 3.64 (dd, J = 10.4, 2.9 Hz, 1H), 3.09 (s, 3H), 2.99 (s, 3H), 2.70–2.65 (m, 2H), 2.41 (s, 1H), 2.12–2.05 (m, 3H), 2.01–1.95 (m, 1H), 1.81–1.75 (m, 1H), 1.68 (s, 3H), 1.45 (s, 3H), 1.24 (s, 3H), 1.11 (s, 3H), 0.99 (s, 3H), 0.95 (d, J = 6.8 Hz, 3H), 0.83 (dd, J = 8.7, 6.9 Hz, 6H). ^{13}C NMR (101 MHz, DMSO) δ 174.58, 170.72, 170.15, 169.16, 168.17, 148.00, 140.24, 138.44, 133.90, 129.46, 128.27, 127.49, 126.51, 125.40, 84.33, 79.15, 72.18, 61.63, 59.97, 59.43, 58.60, 55.61, 50.94, 42.24, 37.58, 31.40, 31.27, 30.13, 29.47, 28.54, 25.08, 24.94, 24.46, 18.27, 15.40, 15.25, 11.20, 10.53, 10.26. HRMS–MALDI (m/z): $[M + Na]^+$ calcd for $C_{41}H_{57}N_3O_{10}Na^+$, 774.3936; found: 774.3940. HPLC purity: 96.0%, t_R = 10.141 min.

*((1R,4S,7R,10S,13S,14R,15E,17E,19R,21S)-4-((S)-sec-Butyl)-10-(2-hydroxypropan-2-yl)-19-methoxy-1,3,14,18-tetramethyl-2,5,8,11-tetraoxo-13-phenyl-12,22-dioxa-3,6,9-triazabicyclo[19.1.0]docosa-15,17-dien-7-yl)methyl cyclopropanecarboxylate (**9m**).* The title compound was synthesized from **8** and cyclopropanecarboxylic acid following the general procedure described for **9e**. Flash column chromatography with hexane and acetone (6 : 1) as eluants afforded the product **9m** in 60% yield as a white solid. ^{1}H NMR (400 MHz, $CDCl_3$) δ 7.34 (d, J = 12.9 Hz, 4H), 7.28 (s, 1H), 6.99 (d, J = 6.6 Hz, 1H), 6.84 (d, J = 9.0 Hz, 1H), 6.39–6.30 (m, 1H), 6.14 (d, J = 10.6 Hz, 1H), 5.99 (s, 1H), 5.91 (dd, J = 15.3, 4.4 Hz, 1H), 4.71 (d, J = 8.8 Hz, 2H), 4.54 (d, J = 11.4 Hz, 1H), 4.22 (d, J = 5.4 Hz, 1H), 3.68 (d, J = 9.7 Hz, 1H), 3.18 (s, 3H), 3.11 (s, 3H), 3.00 (d, J = 9.9 Hz, 1H), 2.68 (s, 1H), 2.60 (s, 1H), 2.18–2.08 (m, 2H), 1.75 (s, 3H), 1.60 (d, J = 9.1 Hz, 1H) 1.53 (s,3H), 1.25 (s, 6H), 1.18 (s, 3H), 1.09 (d, J = 6.7 Hz, 3H), 0.95 (s, 2H), 0.86 (dd, J = 18.6, 12.8 Hz, 9H).^{13}C NMR (101 MHz, $CDCl_3$) δ 174.51, 170.95, 170.25, 169.16, 168.14, 138.65, 136.39, 134.13, 129.27, 128.35, 127.97, 126.74, 126.20, 84.60, 80.33, 72.58, 63.96, 61.93, 60.75, 60.14, 58.80, 55.96, 52.03, 42.00, 31.81, 31.46, 30.12, 29.83, 27.35, 26.43, 24.50, 15.65, 15.52, 12.75, 11.24, 10.77, 10.67, 9.02. HRMS–MALDI (m/z): $[M + Na]^+$ calcd for $C_{40}H_{57}N_3O_{10}Na^+$, 762.3936; found: 762.3940. HPLC purity: 95.5%, t_R = 8.740 min.

*((1R,4S,7R,10S,13S,14R,15E,17E,19R,21S)-4-((S)-sec-Butyl)-10-(2-hydroxypropan-2-yl)-19-methoxy-1,3,14,18-tetramethyl-2,5,8,11-tetraoxo-13-phenyl-12,22-dioxa-3,6,9-triazabicyclo[19.1.0]docosa-15,17-dien-7-yl)methyl 7-(diethylamino)-2-oxo-2H-chromene-3-carboxylate (**9n**).* The title compound was synthesized from **8** and 7-diethylaminocoumarin-3-carboxylic acid following the general procedure described for **9e**. Flash column chromatography with hexane and acetone (5 : 1) as eluants afforded the product **9n** in 90% yield as a yellow solid. ^{1}H NMR (400 MHz, $CDCl_3$) δ 8.51 (s, 1H), 7.80 (d, J = 9.8 Hz, 1H), 7.41–7.35 (m, 6H), 6.62 (d, J = 9.2 Hz, 1H), 6.45–6.35 (m, 1H), 6.34 (d, J = 14.1 Hz, 1H), 6.16 (s, 1H), 6.16 (s, 1H), 6.14 (s, 1H), 6.02–5.97 (m, 1H), 4.94 (d, J = 9.8 Hz, 1H), 4.68 (d, J = 6.5 Hz, 1H), 4.61 (d, J = 11.4 Hz, 1H), 3.91 (t, J = 11.6 Hz, 1H), 3.68 (d, J = 10.3 Hz, 1H), 3.56 (s, 1H), 3.46–3.41 (m, 3H), 3.19–3.15 (m, 4H), 3.09 (s, 3H), 3.00 (d, J = 10.5 Hz, 1H), 2.75 (s, 1H), 1.77 (s, 3H), 1.63 (s, 6H), 1.51 (s, 3H), 1.29–1.20 (m, 6H), 1.18 (s, 3H), 1.08 (d, J = 6.3 Hz, 3H), 0.91 (d, J = 9.1 Hz, 6H). ^{13}C NMR (101 MHz, $CDCl_3$) δ 170.92, 169.93, 168.76, 168.17, 164.08, 159.76, 158.73, 153.57, 151.23, 139.12, 137.15, 133.87, 131.62, 130.23, 128.32, 127.48, 126.84, 126.40, 125.76, 110.26, 108.24, 96.81, 85.07, 79.56, 72.66, 63.76, 61.99, 61.04, 60.62, 58.61, 55.75, 51.27, 45.36, 41.89, 31.88, 31.10, 29.98,

29.84, 27.67, 27.26, 26.78, 15.79, 12.53, 10.66, 9.99. HRMS–ESI (m/z): $[M + H]^+$ calcd for $C_{50}H_{66}N_4O_{12}H^+$, 915.4750; found: 915.4750. HPLC purity: 95.8%, t_R = 8.807 min.

Biology

Cell culture. HCT-116 and HCT-8 cells were purchased from Procell (Wuhan, China) and cultured in a RPMI-1640 medium (Thermo Fisher Scientific, MA, USA) supplemented with 10% fetal bovine serum (FBS, ExCell Bio, Shanghai, China). MDA-MB231 cells were purchased from Procell (Wuhan, China) and maintained in Dulbecco's modified Eagle's medium (DMEM, Thermo Fisher Scientific, MA, USA) supplemented with 10% FBS.

CCK-8 assay. Cell viability was assessed by a cell counting kit-8 (CCK-8) assay (C0042, Beyotime, China). For this, 5×10^3 cells were seeded into 96-well plates for 24 hours. After treatment with different concentrations of nannocystin derivatives for 72 h, the cells were incubated with 10 μL CCK-8 solution per well for 1 h. The absorbance at a wavelength of 450 nm was detected using a Microplate Photometer (Thermo Fisher Scientific, MA, USA) for further IC_{50} analysis.

Cellular uptake. First, 6×10^4 MDA-MB231 cells were seeded into cell slides for 24 h. Then, the concentration-dependent uptake experiment was carried out by incubating MDA-MB231 cells with 0 nM, 250 nM, 500 nM, 1 μM, or 2 μM of **9n** for 1 h followed by the time-dependent uptake experiment conducted by incubating MDA-MB231 cells with 1 μM of **9n** for 0 min, 10 min, 20 min, 40 min, or 60 min. After washing twice with PBS, the cells were fixed with 4% formaldehyde for 2 min, mounted with a mounting fluid, and then observed using a laser scanning confocal microscope (Leica, TCS SP8, Wetzlar, Germany).

Subcellular localization. First, 4×10^4 HCT-8 and MDA-MB231 cells were seeded into cell slides for 24 h and treated with **9n** for 8 h at a concentration of 250 nM and 500 nM, respectively. Then, the cells were washed with HBSS and incubated with ER-Tracker Red (C1041, Beyotime, China) for 20 min at 37 °C. After washing twice with a cell culture medium, the cells were fixed with 4% formaldehyde for 2 min, mounted with a mounting fluid, and then observed using a laser scanning confocal microscope (Leica, TCS SP8, Wetzlar, Germany).

Author contributions

Han Zhang: investigation, visualization, formal analysis. Yunfeng Tian: investigation. Xiaoya Yuan: investigation, visualization, validation. Fei Xie: investigation, visualization. Siqi Yu: investigation, methodology. Jiayou Cai: validation. Bin Sun: resources. Changliang Shan: supervision, funding acquisition, review & editing. Weicheng Zhang: conceptualization, supervision, funding acquisition, writing – original draft, review & editing.

Conflicts of interest

A patent was filed on behalf of Nankai University.

Acknowledgements

We thank helpful discussions with Professor Yue Chen. This work was generously supported by the National Natural Science Foundation of China (NNSFC) (No. 21772101) to W. Zhang, and the National Natural Science Foundation of China (NNSFC) (No. 81973356) to C. Shan.

Notes and references

1 E. M. Driggers, S. P. Hale, J. Lee and N. K. Terrett, *Nat. Rev. Drug Discovery*, 2008, **7**, 608–624.
2 E. Marsault and M. L. Peterson, *J. Med. Chem.*, 2011, **54**, 1961–2004.
3 F. Giordanetto and J. Kihlberg, *J. Med. Chem.*, 2014, **57**, 278–295.
4 H. Van Hattum and H. Waldmann, *J. Am. Chem. Soc.*, 2014, **136**, 11853–11859.
5 G. S. Cremosnik, J. Liu and H. Waldmann, *Nat. Prod. Rep.*, 2020, **37**, 1497–1510.
6 H. Itoh and M. Inoue, *Chem. Rev.*, 2019, **119**, 10002–10031.
7 J. C. Collins and K. James, *MedChemComm*, 2012, **3**, 1489–1495.
8 B. Hong, T. Luo and X. Lei, *ACS Cent. Sci.*, 2020, **6**, 622–635.
9 K. E. Kim, A. N. Kim, C. J. McCormick and B. M. Stoltz, *J. Am. Chem. Soc.*, 2021, **143**, 16890–16901.
10 C. Hardman, S. Ho, A. Shimizu, Q. Luu-Nguyen, J. L. Sloane, M. S. A. Soliman, M. D. Marsden, J. A. Zack and P. A. Wender, *Nat. Commun.*, 2020, **11**, 1879.
11 K. C. Nicolaou, G. Y. C. Leung, D. H. Dethe, R. Guduru, Y.-P. Sun, C. S. Lim and D. Y. K. Chen, *J. Am. Chem. Soc.*, 2008, **130**, 10019–10023.
12 V. R. Ravu, G. Y. C. Leung, C. S. Lim, S. Y. Ng, R. J. Sum and D. Y. K. Chen, *Eur. J. Org. Chem.*, 2011, 463–468.
13 K. C. Nicolaou, D. Rhoades, Y. Wang, R. Bai, E. Hamel, M. Aujay, J. Sandoval and J. Gavrilyuk, *J. Am. Chem. Soc.*, 2017, **139**, 7318–7334.
14 T. Seiser, F. Kamena and N. Cramer, *Angew. Chem., Int. Ed.*, 2008, **47**, 6483–6485.
15 Y. Ying, Y. Liu, S. R. Byeon, H. Kim, H. Luesch and J. Hong, *Org. Lett.*, 2008, **10**, 4021–4024.
16 A. A. Bowers, N. West, T. L. Newkirk, A. E. Troutman-Youngman, S. L. Schreiber, O. Wiest, J. E. Bradner and R. M. Williams, *Org. Lett.*, 2009, **11**, 1301–1304.
17 H. M. Key and S. J. Miller, *J. Am. Chem. Soc.*, 2017, **139**, 15460–15466.
18 R. J. Scamp, E. deRamon, E. K. Paulson, S. J. Miller and J. A. Ellman, *Angew. Chem., Int. Ed.*, 2020, **59**, 890–895.
19 Z. Meng, L. Souillart, B. Monks, N. Huwyler, J. Herrmann, R. Mueller and A. Furstner, *J. Org. Chem.*, 2018, **83**, 6977–6994.
20 H. Hoffmann, H. Kogler, W. Heyse, H. Matter, M. Caspers, D. Schummer, C. Klemke-Jahn, A. Bauer, G. Penarier, L.

Debussche and M. Bronstrup, *Angew. Chem., Int. Ed.*, 2015, **54**, 10145–10148.
21 P. Krastel, S. Roggo, M. Schirle, N. T. Ross, F. Perruccio, P. Aspesi, Jr., T. Aust, K. Buntin, D. Estoppey, B. Liechty, F. Mapa, K. Memmert, H. Miller, X. Pan, R. Riedl, C. Thibaut, J. Thomas, T. Wagner, E. Weber, X. Xie, E. K. Schmitt and D. Hoepfner, *Angew. Chem., Int. Ed.*, 2015, **54**, 10149–10154.
22 W. Zhang, *Molecules*, 2020, **25**, 5327.
23 Y. Tian, X. Xu, Y. Ding, X. Hao, Y. Bai, Y. Tang, X. Zhang, Q. Li, Z. Yang, W. Zhang and Y. Chen, *Eur. J. Med. Chem.*, 2018, **150**, 626–632.
24 Y. Tian, Y. Ding, X. Xu, Y. Bai, Y. Tang, X. Hao, W. Zhang and Y. Chen, *Tetrahedron Lett.*, 2018, **59**, 3206–3209.
25 Y. Tian, J. Wang, W. Liu, X. Yuan, Y. Tang, J. Li, Y. Chen and W. Zhang, *J. Mol. Struct.*, 2019, **1181**, 568–578.
26 Q. Liu, X. Yang, J. Ji, S.-L. Zhang and Y. He, *Eur. J. Med. Chem.*, 2019, **170**, 99–111.
27 An alternative and perhaps a more cutting-edge strategy is to invoke site-selective functionalization of an intricate structure by means of enabling catalysts. For recent leading reviews, see ref. 28–33.
28 O. Robles and D. Romo, *Nat. Prod. Rep.*, 2014, **31**, 318–334.
29 T. Cernak, K. D. Dykstra, S. Tyagarajan, P. Vachal and S. W. Krska, *Chem. Soc. Rev.*, 2016, **45**, 546–576.
30 C. R. Shugrue and S. J. Miller, *Chem. Rev.*, 2017, **117**, 11894–11951.
31 W. Wang, M. M. Lorion, J. Shah, A. R. Kapdi and L. Ackermann, *Angew. Chem., Int. Ed.*, 2018, **57**, 14700–14717.
32 L. Guillemard, N. Kaplaneris, L. Ackermann and M. J. Johansson, *Nat. Rev. Chem.*, 2021, **5**, 522–545.
33 E. Romero, B. S. Jones, B. N. Hogg, A. Rue Casamajo, M. A. Hayes, S. L. Flitsch, N. J. Turner and C. Schnepel, *Angew. Chem., Int. Ed.*, 2021, **60**, 16824–16855.
34 M. Tsakos, E. S. Schaffert, L. L. Clement, N. L. Villadsen and T. B. Poulsen, *Nat. Prod. Rep.*, 2015, **32**, 605–632.
35 K. C. Nicolaou, C. Nilewski, C. R. H. Hale, C. F. Ahles, C. A. Chiu, C. Ebner, A. ElMarrouni, L. Yang, K. Stiles and D. Nagrath, *J. Am. Chem. Soc.*, 2015, **137**, 4766–4770.
36 M. H. Nguyen, M. Imanishi, T. Kurogi, X. Wan, J. E. Ishmael, K. L. McPhail and A. B. Smith, *J. Org. Chem.*, 2018, **83**, 4287–4306.
37 B. E. Alexander, S. Sun, M. J. Palframan, G. Kociok-Koehn, D. F. Dibwe, S. Watanabe, L. Caggiano, S. Awale and S. E. Lewis, *ChemMedChem*, 2020, **15**, 125–135.
38 C. S. M. Amrine, A. C. Huntsman, M. G. Doyle, J. E. Burdette, C. J. Pearce, J. R. Fuchs and N. H. Oberlies, *ACS Med. Chem. Lett.*, 2021, **12**, 625–630.
39 K. Zhang, W. Song, M. Wei, Y. Sun, N. Wang, L. Ma, X. Yu, R. Gao, R. Wang, Y. Zhang, N. Zheng, N. Li, L. Mu, Z. Tang, X. Li, C. Yang and G. Yang, *J. Med. Chem.*, 2021, **64**, 15825–15845.
40 Y.-F. Zhou, B.-C. Yan, Q. Yang, X.-Y. Long, D.-Q. Zhang, R.-H. Luo, H.-Y. Wang, H.-D. Sun, X.-S. Xue, Y.-T. Zheng and P.-T. Puno, *Angew. Chem., Int. Ed.*, 2022, **61**, e202201684.
41 C. Sun, R. Liu, M. Xia, Y. Hou, X. Wang, J.-J. Lu, B. Liu and X. Chen, *Toxicol. Appl. Pharmacol.*, 2021, **420**, 115535.
42 Y. Hou, R. Liu, M. Xia, C. Sun, B. Zhong, J. Yu, N. Ai, J.-J. Lu, W. Ge, B. Liu and X. Chen, *Pharmacol. Res.*, 2021, **173**, 105870.
43 Z. Yang, X. Xu, C. H. Yang, Y. Tian, X. Chen, L. Lian, W. Pan, X. Su, W. Zhang and Y. Chen, *Org. Lett.*, 2016, **18**, 5768–5770.
44 W. Zhang, *Nat. Prod. Rep.*, 2021, **38**, 1109–1135.
45 D. Paul, S. Das, S. Saha, H. Sharma and R. K. Goswami, *Eur. J. Org. Chem.*, 2021, 2057–2076.
46 S. Das, D. Paul and R. K. Goswami, *Org. Lett.*, 2016, **18**, 1908–1911.
47 M. H. Nguyen, M. Imanishi, T. Kurogi and A. B. Smith, *J. Am. Chem. Soc.*, 2016, **138**, 3675–3678.
48 D. Paul, S. Das and R. K. Goswami, *J. Org. Chem.*, 2017, **82**, 7437–7445.
49 D. Meidlinger, L. Marx, C. Bordeianu, S. Choppin, F. Colobert and A. Speicher, *Angew. Chem., Int. Ed.*, 2018, **57**, 9160–9164.
50 D. Paul, M. H. Sahana, P. Mandal, P. Chakrabarti and R. K. Goswami, *Org. Biomol. Chem.*, 2020, **18**, 7151–7164.
51 L. Fritz, S. Wienhold, S. Hackl and T. Bach, *Chem. – Eur. J.*, 2022, **28**, e202104064.
52 W. Abbas, A. Kumar and G. Herbein, *Front. Oncol.*, 2015, **5**, 75.
53 A. N. Sasikumar, W. B. Perez and T. G. Kinzy, *Wiley Interdiscip. Rev. RNA*, 2012, **3**, 543–555.
54 G. S. Hussey, A. Chaudhury, A. E. Dawson, D. J. Lindner, C. R. Knudsen, M. C. J. Wilce, W. C. Merrick and P. H. Howe, *Mol. Cell*, 2011, **41**, 419–431.
55 S. Liu, S. Hausmann, S. M. Carlson, M. E. Fuentes, J. W. Francis, R. Pillai, S. M. Lofgren, L. Hulea, K. Tandoc, J. Lu, A. Li, N. D. Nguyen, M. Caporicci, M. P. Kim, A. Maitra, H. Wang, I. I. Wistuba, J. A. Porco, Jr., M. C. Bassik, J. E. Elias, J. Song, I. Topisirovic, C. Van Rechem, P. K. Mazur and O. Gozani, *Cell*, 2019, **176**, 491–504.
56 A. Amiri, F. Noei, S. Jeganathan, G. Kulkarni, D. E. Pinke and J. M. Lee, *Oncogene*, 2007, **26**, 3027–3040.
57 N. Elgohary, R. Pellegrino, O. Neumann, H. M. Elzawahry, M. M. Saber, A. A. Zeeneldin, R. Geffers, V. Ehemann, P. Schemmer, P. Schirmacher and T. Longerich, *Int. J. Oncol.*, 2015, **46**, 597–606.
58 L. Jia, X. Ge, C. Du, L. Chen, Y. Zhou, W. Xiong, J. Xiang, G. Li, G. Xiao, L. Fang and Z. Li, *Br. J. Cancer*, 2021, **124**, 1301–1311.
59 J. G. Moffat, F. Vincent, J. A. Lee, J. Eder and M. Prunotto, *Nat. Rev. Drug Discovery*, 2017, **16**, 531–543.
60 F. Vincent, A. Nueda, J. Lee, M. Schenone, M. Prunotto and M. Mercola, *Nat. Rev. Drug Discovery*, 2022, **21**, 899–914.
61 J.-U. Peters, *J. Med. Chem.*, 2013, **56**, 8955–8971.
62 A. Anighoro, J. Bajorath and G. Rastelli, *J. Med. Chem.*, 2014, **57**, 7874–7887.
63 M. Kibble, N. Saarinen, J. Tang, K. Wennerberg, S. Mäkelä and T. Aittokallio, *Nat. Prod. Rep.*, 2015, **32**, 1249–1266.
64 P. C. Jimenez, D. V. Wilke, P. C. Branco, A. Bauermeister, P. Rezende-Teixeira, S. P. Gaudencio and L. V. Costa-Lotufo, *Br. J. Pharmacol.*, 2020, **177**, 3–27.

65 A. Losada, M. J. Munoz-Alonso, C. Garcia, P. A. Sanchez-Murcia, J. F. Martinez-Leal, J. M. Dominguez, M. P. Lillo, F. Gago and C. M. Galmarini, *Sci. Rep.*, 2016, **6**, 35100.

66 A. Losada, M. J. Munoz-Alonso, M. Martinez-Diez, F. Gago, J. M. Dominguez, J. F. Martinez-Leal and C. M. Galmarini, *Br. J. Cancer*, 2018, **119**, 1410–1420.

67 M. B. Potts, E. A. McMillan, T. I. Rosales, H. S. Kim, Y.-H. Ou, J. E. Toombs, R. A. Brekken, M. D. Minden, J. B. MacMillan and M. A. White, *Nat. Chem. Biol.*, 2015, **11**, 401–408.

68 S. B. Wagh, V. A. Maslivetc, J. J. La Clair and A. Kornienko, *ChemBioChem*, 2021, **22**, 3109–3139.

69 L. D. Lavis and R. T. Raines, *ACS Chem. Biol.*, 2014, **9**, 855–866.

70 M. D. Alexander, M. D. Burkart, M. S. Leonard, P. Portonovo, B. Liang, X. Ding, M. M. Joullie, B. M. Gulledge, J. B. Aggen, A. R. Chamberlin, J. Sandler, W. Fenical, J. Cui, S. J. Gharpure, A. Polosukhin, H.-R. Zhang, P. A. Evans, A. D. Richardson, M. K. Harper, C. M. Ireland, B. G. Vong, T. P. Brady, E. A. Theodorakis and J. J. La Clair, *ChemBioChem*, 2006, **7**, 409–416.

71 S. Xu, S. Luo, H. Yao, H. Cai, X. Miao, F. Wu, D.-H. Yang, X. Wu, W. Xie, H. Yao, Z.-S. Chen and J. Xu, *J. Med. Chem.*, 2016, **59**, 5022–5034.

72 H. Yao, G. Wei, Y. Liu, H. Yao, Z. Zhu, W. Ye, X. Wu, J. Xu and S. Xu, *ACS Med. Chem. Lett.*, 2018, **9**, 1030–1034.

73 T. Zhu, C. Chen, S. Wang, Y. Zhang, D. Zhu, L. Li, J. Luo and L. Kong, *Chem. Commun.*, 2019, **55**, 8231–8234.

74 C. C. Hughes, J. B. MacMillan, S. P. Gaudencio, W. Fenical and J. J. La Clair, *Angew. Chem., Int. Ed.*, 2009, **48**, 728–732.

75 W.-L. Yu, B. D. Jones, M. Kang, J. C. Hammons, J. J. La Clair and M. D. Burkart, *J. Nat. Prod.*, 2013, **76**, 817–823.

76 L. Trzoss, T. Fukuda, L. V. Costa-Lotufo, P. Jimenez, J. J. La Clair and W. Fenical, *Proc. Natl. Acad. Sci. U. S. A.*, 2014, **111**, 14687–14692.

77 H.-Y. Wang, H. Yang, M. Holm, H. Tom, K. Oltion, A. A. Q. Al-Khdhairawi, J.-F. F. Weber, S. C. Blanchard, D. Ruggero and J. Taunton, *Nat. Chem.*, 2022, **14**, 1443–1450.

78 C. Liu, L. Wang, Y. Sun, X. Zhao, T. Chen, X. Su, H. Guo, Q. Wang, X. Xi, Y. Ding and Y. Chen, *Angew. Chem., Int. Ed.*, 2022, **61**, e202206953.

79 V. G. Klein, W. M. Bray, H.-Y. Wang, Q. Edmondson, J. Schwochert, S. Ono, M. R. Naylor, A. C. Turmon, J. H. Faris, O. Okada, J. Taunton and R. S. Lokey, *ACS Chem. Biol.*, 2021, **16**, 1354–1364.

80 P. Portonovo, X. Ding, M. S. Leonard and M. M. Joullié, *Tetrahedron*, 2000, **56**, 3687–3690.

81 M. M. Joullié, M. S. Leonard, P. Portonovo, B. Liang, X. Ding and J. J. La Clair, *Bioconjugate Chem.*, 2003, **14**, 30–37.

82 W. C. Merrick and J. Nyborg, *Cold Spring Harbor Monogr. Ser.*, 2000, **39**, 89–126.

83 D. N. Itzhak, S. Tyanova, J. Cox and G. H. H. Borner, *eLife*, 2016, **5**, e16950.

84 D. N. Hebert and M. Molinari, *Physiol. Rev.*, 2007, **87**, 1377–1408.

85 D. W. Reid and C. V. Nicchitta, *Nat. Rev. Mol. Cell Biol.*, 2015, **16**, 221–231.

86 J. Sanders, M. Brandsma, G. M. C. Janssen, J. Dijk and W. Moeller, *J. Cell Sci.*, 1996, **109**, 1113–1117.

87 S. Kjær, T. Wind, P. Ravn, M. Østergaard, B. F. C. Clark and A. Nissim, *Eur. J. Biochem.*, 2001, **268**, 3407–3415.

88 A. M. Stoianov, D. L. Robson, A. M. Hetherington, C. G. Sawyez and N. M. Borradaile, *PLoS One*, 2015, **10**, e0131269.

89 S. Thornton, N. Anand, D. Purcell and J. Lee, *J. Mol. Med.*, 2003, **81**, 536–548.

90 M. K. Mateyak and T. G. Kinzy, *J. Biol. Chem.*, 2010, **285**, 21209–21213.

91 K. M. White, R. Rosales, S. Yildiz, T. Kehrer, L. Miorin, E. Moreno, S. Jangra, M. B. Uccellini, R. Rathnasinghe, L. Coughlan, C. Martinez-Romero, J. Batra, A. Rojc, M. Bouhaddou, J. M. Fabius, K. Obernier, M. Dejosez, M. Jose Guillen, A. Losada, P. Aviles, M. Schotsaert, T. Zwaka, M. Vignuzzi, K. M. Shokat, N. J. Krogan and A. Garcia-Sastre, *Science*, 2021, **371**, 926–931.